August 2013

Thesis for Master Degree

Oleanane triterpenes from *Camellia japonica* inhibit growth of breast cancer cell lines via PTP1B inhibition

Chosun University Graduate School

College of Pharmacy

Uddin Mohammad Nasir

Oleanane triterpenes from *Camellia japonica* inhibit growth of breast cancer cell lines via PTP1B inhibition

동백나무로부터 분리한 올레안계 화합물의 PTP1B 효소 저해를 경유한 유방암 세포주 저해활성 연구

2013년 08월 23일

`

Chosun University Graduate School

College of Pharmacy

Uddin Mohammad Nasir

Oleanane triterpenes from *Camellia japonica* inhibit growth of breast cancer cell lines via PTP1B inhibition

지도교수 최 홍 석

공동지도교수 오 원 근

이 논문을 약학 석사학위신청 논문으로 제출함

2013년 04월

조선대학교 대학원

약학대학

우딘 모함마드 나시르

This thesis is examined and approved for Uddin Mohammad Nasir's master degree

Chairman Chosun Univ. Prof. Choi Hoo Kyun (인)

Member Seoul National Univ. Prof. Kang Keon Wook (인)

Member Chosun Univ. Prof. Choi Hong Seok (인)

2013년 05월

Chosun University Graduate School

Contents

Contents …….. **i**

List of Schemes …….. **iii**

List of Tables …….. **iv**

List of Figures …… **v**

List of Abbreviations …… **viii**

Abstract …….. **x**

Korean ……. x

English ……. xii

1. Introduction …… **1**

1.1. Breast cancer ……... 1

1.2. PTP1B …… 3

1.3. PTP1B role in breast cancer ……... 6

1.4. Plant triterpenoids …….. 7

1.5. Triterpenoids and breast cancer …….. 8

1.6. *Camellia japonica* L. (Theaceae) ……... 11

2. Materials and Methods …….. **13**

2.1. **Materials ……...** **13**

2.1.1. Plant material …… 13

2.1.2. Chemicals, reagents and chromatography …… 13

2.1.3. General experimental procedures ……. 14

2.2. **Methods ……..** **14**

2.2.1. Extraction and isolation …… 14

2.2.2. PTP1B inhibition assay …… 20

2.2.3. Kinetic parameters for PTP1B inhibition type ……. 20

2.2.4. Cell culture ……... 20

2.2.5. MTT cytotoxicity assay …… 21

2.2.6. Statistical analysis …… 21

3. Results and Discussions …….. 22

3.1. Structural determination of new compounds **1**-**6** ……... 22

3.1.1. Structural determination of compound **1** …….. 22

3.1.2. Structural determination of compound **2** …….. 28

3.1.3. Structural determination of compound **3** …….. 34

3.1.4. Structural determination of compound **4** …….. 40

3.1.5. Structural determination of compound **5** …….. 46

3.1.6. Structural determination of compound **6** …….. 52

3.2. PTP1B inhibitory effects of isolated compounds **1**-**14** …….. 57

3.3. PTP1B inhibition mode for isolated compounds-Lineweaver-Burk and Dixon plots ……. 60

3.4. Growth inhibitory effects of isolated compounds (**1**-**14**) against breast cancer cell lines …….. 62

3.5. Structure activity relationships ……... 65

4. Conclusions …… 66

5. References …… 67

6. Acknowledgements ……. 79

List of Schemes

Scheme 1. Isolation of new compounds (**1**–**6**) from *C. japonica* ……... 17

List of Tables

Table 1. ^{1}H (500 MHz) and ^{13}C (125 MHz) -NMR data of compound **1** in $CDCl_3$ …... 27

Table 2. ^{1}H (500 MHz) and ^{13}C (125 MHz) -NMR data of compound **2** in $CDCl_3$ …... 33

Table 3. ^{1}H (500 MHz) and ^{13}C (125 MHz) -NMR data of compound **3** in acetone-d_6 . 39

Table 4. ^{1}H (500 MHz) and ^{13}C (125 MHz) -NMR data of compound **4** in $CDCl_3$ …... 45

Table 5. ^{1}H (500 MHz) and ^{13}C (125 MHz) -NMR data of compound **5** in acetone-d_6 . 51

Table 6. ^{1}H (600 MHz) and ^{13}C (150 MHz) -NMR data of compound **6** in acetone-d_6 . 56

Table 7. Inhibitory effects of isolated compounds **1-14** on PTP1B enzyme …….. 58

Table 8. Growth inhibitory effects of isolated compounds (**1-14**) against breast cancer cell lines ……... 63

List of Figures

Fig. 1. Mechanism of action of tamoxifen and aromatase inhibitors …….. 2

Fig. 2. Structural features of PTP1B as a ribbon diagram …….. 4

Fig. 3. PTP1B as a negative regulator of multiple signaling pathways …….. 5

Fig. 4. Triterpenes with therapeutic potential in breast cancer ……... 10

Fig. 5. *Camellia japonica* L. (**A**) Flower; (**B**) Fruit; (**C**) Fruit peel ……... 11

Fig. 6. Chemical structures of compounds **1**-**14** isolated from *Camellia japonica* ……. 19

Fig. 7. Key HMBC (H→C) correlations of compound **1** …… 23

Fig. 8. ^{1}H-NMR ($CDCl_3$ 500 MHz) spectrum of compound **1** ……... 24

Fig. 9. ^{13}C-NMR ($CDCl_3$ 125 MHz) spectrum of compound **1** …….. 24

Fig. 10. HMBC spectrum of compound **1** ……... 25

Fig. 11. HSQC spectrum of compound **1** …… 25

Fig. 12. EIMS spectrum of compound **1** ……. 26

Fig. 13. IR (KBr) spectrum of compound **1** ……... 26

Fig. 14. Key HMBC (H→C) and NOESY (H⇢H) correlations of compound **2**…….. 29

Fig. 15. ^{1}H-NMR ($CDCl_3$ 500 MHz) spectrum of compound **2** ……. 30

Fig. 16. ^{13}C-NMR ($CDCl_3$ 125 MHz) spectrum of compound **2** …… 30

Fig. 17. HMBC spectrum of compound **2** ……... 31

Fig. 18. HSQC spectrum of compound **2** …… 31

Fig. 19. EIMS spectrum of compound **2** ……. 32

Fig. 20. ^{1}H-^{1}H- NOESY spectrum of compound **2** ……. 32

Fig. 21. Key HMBC (H→C) and NOESY (H⇢H) correlations of compound **3** ……. 35

Fig. 22. ^{1}H-NMR (acetone-d_6 500 MHz) spectrum of compound **3** ……... 36

Fig. 23. ^{13}C-NMR (acetone-d_6 125 MHz) spectrum of compound **3** …….. 36

Fig. 24. HMBC spectrum of compound **3** ……... 37

Fig. 25. HSQC spectrum of compound **3** …… 37

Fig. 26. FABMS spectrum of compound **3** ……. 38

Fig. 27. ^{1}H-^{1}H- NOESY spectrum of compound **3** ……. 38

Fig. 28. Key HMBC (H→C) and NOESY (H⇢H) correlations of compound **4** ……. 41

Fig. 29. ^{1}H-NMR ($CDCl_3$ 500 MHz) spectrum of compound **4** ……. 41

Fig. 30. ^{13}C-NMR ($CDCl_3$ 125 MHz) spectrum of compound **4** …… 42

Fig. 31. HMBC spectrum of compound **4** ……... 42

Fig. 32. HSQC spectrum of compound **4** …… 43

Fig. 33. FABMS spectrum of compound **4** ……. 43

Fig. 34. ^{1}H-^{1}H- NOESY spectrum of compound **4** ……. 44

Fig. 35. IR (KBr) spectrum of compound **4** ……... 44

Fig. 36. Key HMBC (H→C) correlation of compound **5** ……... 48

Fig. 37. ^{1}H-NMR (acetone-d_6 500 MHz) spectrum of compound **5** ……... 48

Fig. 38. ^{13}C-NMR (acetone-d_6 125 MHz) spectrum of compound **5** …….. 49

Fig. 39. HMBC spectrum of compound **5** ……... 49

Fig. 40. HSQC spectrum of compound **5** …… 50

Fig. 41. FABMS spectrum of compound **5** ……. 50

Fig. 42. Key HMBC (H→C) correlation of compound **6** ……... 53

Fig. 43. ^{1}H-NMR (acetone-d_6 600 MHz) spectrum of compound **6** ……... 53

Fig. 44. ^{13}C-NMR (acetone-d_6 150 MHz) spectrum of compound **6** …….. 54

Fig. 45. HMBC spectrum of compound **6** ……... 54

Fig. 46. HSQC spectrum of compound **6** …… 55

Fig. 47. FABMS spectrum of compound **6** ……. 55

Fig. 48. PTP1B inhibitory effects of the isolated compounds from *C. japonica*. Compounds **2**, **8**, **10, 11,** and **13** showed concentration dependent strong inhibition on PTP1B activity. Ursolic acid was used as positive control which was presented in Table 7. Compound concentrations are displayed on logarithmic scales …… 59

Fig. 49. Graphical determination of inhibition mode for the isolated compounds. (**A-B**) Lineweaver-Burk plots for the inhibition of compounds **2** and **11** on the PTP1B-catalyzed hydrolysis of *p*-NPP. The data are expressed as the mean reciprocal of initial velocity for $n = 3$ replicates at each substrate concentration. (**C-D**) Dixon plots for compounds **2** and **11** determining the inhibition constant K_i. The K_i value was determined from the negative *x*-axis value at the point of the intersection of the five lines. The data are expressed as the mean reciprocal of initial velocity for $n = 3$ replicates at each substrate concentration ……... 61

Fig. 50. Growth inhibitory effects of isolated compounds against breast cancer cell lines. Compounds **2, 8, 10, 11,** and **13** showed very strong growth inhibition on (**A**) MCF7 (**B**) MCF7/ADR and (**C**) MDA-MB-231 breast cancer cell lines in a concentration dependent manner. 4-hydroxytamoxifen was used as positive control in all experiments and also presented in Table 8. Concentrations of all compounds are displayed on logarithmic scales. The IC_{50} value was determined from the midpoint (cytotoxic activity = 50%) of the semilog plot …… 64

List of Abbreviations

ADR	adriamycin resistant
DMEM	dulbecco's modified eagle’s medium
DTT	dithiothreitol
EGFR	epidermal growth factor receptor
ER	estrogen receptor
FBS	fetal bovine serum
FT-IR	fourier transformed infra red
HER2	human epidermal growth factor receptor 2
HIV-1	human immunodeficiency virus-1
HMBC	heteronuclear multiple bond correlation
HMQC	heteronuclear multiple quantum coherence
HPLC	high performance liquid chromatography
HREIMS	high resolution electro impact mass spectroscopy
HRFABMS	high resolution fast atom bombardment mass spectroscopy
IC_{50}	50% inhibitory concentration
IGF-IR	insulin-like growth factor 1 receptor
IR	insulin receptor
IR	infra red
IRS	insulin receptor substrates
JAK2	janus kinase 2
m/z	mass to charge ratio
MCF7	michigan cancer foundation - 7

MTT	3-(4, 5-dimethylthiazol-2-yl)-2, 5-diphenyl-tetrazolium bromide
NMR	nuclear magnetic resonance
NOESY	nuclear overhauser effect spectroscopy
OCC	open column chromatography
PDGFR	platelet derived growth factor receptor
PgR	progesterone receptor
p-NPP	para-nitro phenyl phosphate
ppm	parts per million
PTKs	protein tyrosine kinases
PTP1B	protein tyrosine phosphatase 1B
PTPN1	protein tyrosine phosphatase non-receptor type 1
PTPs	protein tyrosine phosphatases
RP	reverse phase
SERM	selective estrogen receptor modulators
STAT3	signal transducer and activator of transcription 3
STAT5	signal transducer and activator of transcription 5
TLC	thin layer chromatography
TYK2	tyrosine kinase 2
UV	ultra violet

(국문 초록)

동백나무로부터 분리한 올레안계 화합물의 PTP1B 효소 저해를 경유한 유방암 세포주 저해활성 연구

우딘 모함마드 나시르
지도교수: 최 홍 석
공동지도교수: 오 원 근
약학대학
조선대학교 대학원

유방암의 심각한 사망률은 화학요법, 방사선요법, 수술을 포함한 현재의 치료방법에 의하여 어느정도 치료되고 있다. 그러므로 새로운 치료방법의 개발은 이러한 심각한 유방암의 치료법에 있어서 중요한 것이다. PTP1B와 유방암 질환의 발병에 관한 최근 연구는 선택적인 PTP1B 저해가 유방암 치료에 중요한 역할을 할수 있다고 제안되고 있다. 흥미롭게도, 강력한 PTP1B 저해제로서 인식되어온 식물기원의 triterpenes 역시 유방암에 대한 치료효과가 있음을 보여주었다. 그러므로 계속적인 triterpenes에 대한 연구로서 8개의 이미 알려진 oleanane-type triterpenes (**7-14**)과 함께 6개의 새로운 oleanane-type triterpenes (**1-6**)계 화합물을 동백나무의 열매껍질 (*Camellia japonica* L.,Theaceae)의 EtOAc분획물로부터 분리하였다. 모든 얻어진 신규 화합물의 화학구조는 물리화학적 방법과 스펙트럼 분석법 (IR, 1D, 2D-NMR, and MS)를 통하여 3,16-dioxo-olean-12(13),17(18)-

diene (**1**), 3β,16α,17-trihydroxy-olean-12-ene (**2**), 4,28,29-trihydroxy-16-oxo-3,4-*seco*-olean-12-ene-3-oic acid methyl ester (Camelliaolean A) (**3**), 4,7β,17-trihydroxy-16-oxo-3,4-*seco*-olean-12-ene-3-oic acid methyl ester (Camelliaolean B) (**4**), 7β,17,29-trihydroxy-16-oxo-3,4-*seco*-olean-4(23),12(13)-diene-3-oic acid methyl ester (Camelliaolean C) (**5**), and 17,29-dihydroxy-16-oxo-3,4-*seco*-olean-4(23),12(13)-diene-3-oic acid (Camelliaolean D) (**6**) 으로 확인하였다. 분리한 화합물 모두에 대하여 MCF7, MCF7/ADR, MDA-MB-231 유방암 세포주에 대한 활성과 in vitro PTP1B효소에 대한 효과가 평가되었다. C-3 hydroxy group이나 C-28 carboxy group을 가진 화합물인 화합물 **2**, **8**, **10**, **11**, 그리고 **13**은 좋은 세포독성 (IC_{50} 수치는 0.51 ± 0.05에서부터 9.32 ± 0.62 μM까지 이른다) 보여주었을 뿐만 아니라 강력한 PTP1B 저해활성 (IC_{50} 수치는 3.77 ± 0.11 에서 6.40 ± 0.81 μM에 이른다)을 보여주었다. 그러나, C-3위치에 ketone기가 결합된 화합물인 화합물 **1**과 **5**는 MCF7, MCF7/ADR, MDA-MB-231 유방암 세포주에 대한 성장 억제효과와 in vitro PTP1B효소에 대한 저해 효과가 감소하였다. 이러한 결과들은 *C. japonica*로부터 분리된 oleanane triterpenes화합물들이 PTP1B 저해제로서 유방암 세포주에 대한 세포독성을 갖는 새로운 화합물로서 가능성을 갖음을 제시한다.

Abstract

Oleanane triterpenes from *Camellia japonica* inhibit growth of breast cancer cell lines via PTP1B inhibition

Uddin Mohammad Nasir

Advisor: Prof. Choi Hong Seok, Ph.D.

Co-Advisor: Prof. Oh Won Keun, Ph.D.

College of Pharmacy,

Graduate School of Chosun University

The significant morbidity of advanced breast cancer has been only somewhat impacted by current treatment modalities including chemotherapy, radiotherapy and surgery. Therefore, development of novel therapeutic approaches would be of interest in combating this disease. Recent studies on PTP1B and breast tumorigenesis suggest that selective PTP1B inhibition might play an important role in breast cancer treatment. Interestingly, plant triterpenes, which have already been appreciated as strong PTP1B inhibitors, also showed therapeutic potential in breast cancer. Therefore, as part of research on triterpenes, six new (**1**-**6**) along with eight known (**7**-**14**) oleanane-type triterpenes were isolated from the EtOAc extract of the fruit peels of *Camellia japonica* L. (Theaceae). The chemical structures of new compounds were elucidated by physicochemical and spectroscopic (IR, 1D, 2D-NMR, and MS) data analysis as 3,16-dioxo-olean-12(13),17(18)-diene (**1**), 3β,16α,17-trihydroxy-olean-12-ene (**2**), 4,28,29-trihydroxy-16-oxo-3,4-*seco*-olean-12-ene-3-oic acid methyl ester (Camelliaolean A) (**3**),

4,7β,17-trihydroxy-16-oxo-3,4-*seco*-olean-12-ene-3-oic acid methyl ester (Camelliaolean B) (**4**), 7β,17,29-trihydroxy-16-oxo-3,4-*seco*-olean-4(23),12(13)-diene-3-oic acid methyl ester (Camelliaolean C) (**5**)**,** and 17,29-dihydroxy-16-oxo-3,4-*seco*-olean-4(23),12(13)-diene-3-oic acid (Camelliaolean D) (**6**). All the isolates were evaluated for their inhibitory effects on PTP1B enzyme, as well as their growth inhibition on MCF7, adriamycin-resistant MCF7 (MCF7/ADR) and MDA-MB-231 breast cancer cell lines. Compounds **2**, **8**, **10**, **11**, and **13** with C-3 hydroxy group or/and C-28 carboxy group showed strong PTP1B inhibitory activity (IC_{50} values ranging from 3.77 ± 0.11 to 6.40 ± 0.81 μM) as well as significant cytotoxicity (IC_{50} values ranging from 0.51 ± 0.05 to 9.32 ± 0.62 μM) while attachment of ketone group at C-3 position reduced both type effects in **1,** and **5**. These results suggested that, oleanane triterpenes from *C. japonica* as PTP1B inhibitors could be considered as new anticancer materials for breast cancer treatment.

1. Introduction

1.1. Breast cancer

Despite advances in treatment**,** breast cancer remains one of the leading causes of cancer death among women worldwide, with an estimated 1 million new cases per year.[1] According to the American cancer society, about 232,340 new cases and 39,620 deaths are estimated to occur in 2013 in women in the United States alone.[2] In the United States, a woman will die from breast cancer every 13 min and over 1 million women have died from this disease since 1970. Surprisingly, the incidence of male breast cancer is also on the rise.[3] In 2013, about 2,240 new cases of breast cancer and 410 deaths are estimated to occur among men in the United States.[2]

Breast cancer is influenced by several hormones, specifically estrogen and progesterone which are well known to be involved in mammary tumorigenesis.[4] Approximately 75-80% of breast cancers are positive for estrogen receptor [ER] or progesterone receptor [PgR] whereas 15-20% are positive for HER2/neu receptor.[5] The remaining 10-15% of breast cancer is in a so-called receptor-negative or triple-negative category, as defined by absent expression of these three proteins.

Estrogen is produced in ovaries in case of premenopausal women while in adipose tissue and adrenal glands in case of postmenopausal women. The enzyme aromatase plays a critical role in the production of estrogen in postmenopausal women. At present, to treat estrogen receptor (ER)-positive breast cancers, several selective estrogen receptor modulators (SERM) have been developed, among which, tamoxifen is being considered as first line treatment choice.[6] Tamoxifen inhibits the growth of breast tumors by competitive antagonism of estrogen at its receptor site (Fig. 1). Its actions are complex, however, and it also has partial

estrogen agonist effects. These partial agonist effects can be beneficial, since they may help prevention of bone demineralization in postmenopausal women,[7] but also detrimental, as they are associated with increased risks of endometrial cancer[8] and thromboembolism.[9] In addition, they may play a part in the development of tamoxifen resistance.[10] In contrast, aromatase inhibitors (e.g. letrozole, anastrozole) markedly suppress plasma estrogen levels in postmenopausal women by inhibiting or inactivating aromatase, the enzyme responsible for the synthesis of estrogens from androgenic substrates (specifically, the synthesis of estrone from the preferred substrate androstenedione and estradiol from testosterone) (Fig. 1). Unlike tamoxifen, aromatase inhibitors have no partial agonist activity.

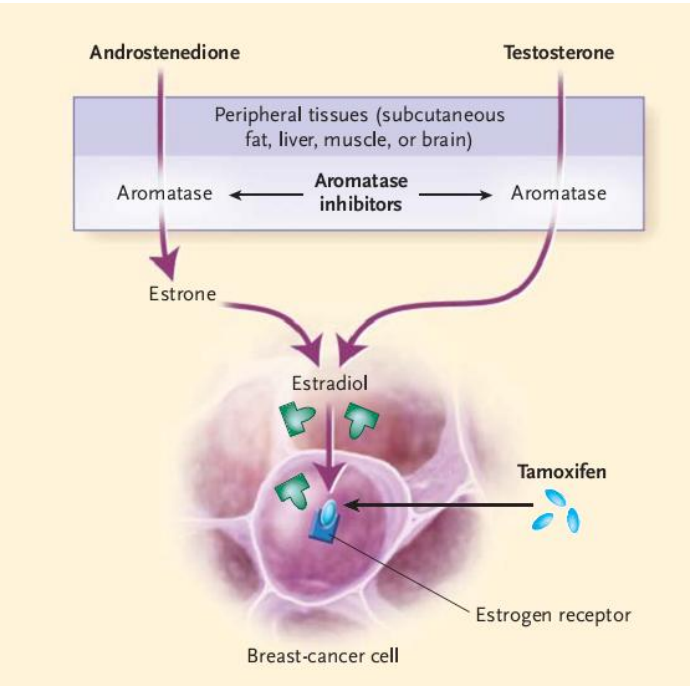

Fig. 1. Mechanism of action of tamoxifen and aromatase inhibitors

Women with breast cancer that overexpresses human epidermal growth factor receptor type 2 (HER2, also referred to as HER2/neu) are at greater risk for disease progression and death than women whose tumors do not overexpress HER2.[11] Therapeutic strategies have been

developed to block HER2 signaling pathways in order to improve the treatment of this cancer. Trastuzumab, a recombinant, humanized, monoclonal antibody that binds to the extracellular domain of the HER2 protein, is being used in HER2/neu-positive breast cancers.[12] However, trastuzumab has potential concern of severe cardiac dysfunction.[13] Therefore, as a alternatives, lapatinib has been developed and found to be effective in delaying disease progression in women with HER2-positive advanced breast cancers that have become resistant to trastuzumab.[14] In addition to these drug therapies, the treatment of breast cancer may also involve surgery (mastectomy, breast conserving surgery) and radiation therapy depending on the tumor size, extent of spread and other characteristics, as well as patient preference.

Unfortunately, the significant morbidity of breast cancer has been only somewhat impacted by current treatment modalities including surgery, radiotherapy, and adjuvant chemotherapy and/or hormone therapies.[15, 16] There is still no effective cure for the vast majority of patients with advanced stages of the disease.[17] Hence, there is a critical and urgent need for developing agents that will be effective in decreasing the incidence of breast cancer in high risk women.

1.2. PTP1B

Reversible protein tyrosine phosphorylation catalyzed by the coordinated actions of protein tyrosine kinases (PTKs) and phosphatases (PTPs) is of paramount importance to the regulation of the signaling events that underlie such fundamental processes as growth and proliferation, differentiation and survival or apoptosis, as well as adhesion and motility.[18] Protein tyrosine phosphatase 1B (PTP1B) is the prototype for the superfamily of PTPs and has been the most extensively studied within the group. This enzyme, named from a pool of PTP activity resolved by ion-exchange chromatography, was originally purified from human

placenta as a 37 kDa catalytic domain.[19] Recently, it has come into focus as an important regulator of various signaling pathways involved in human diseases such as diabetes, obesity, and cancer.[20]

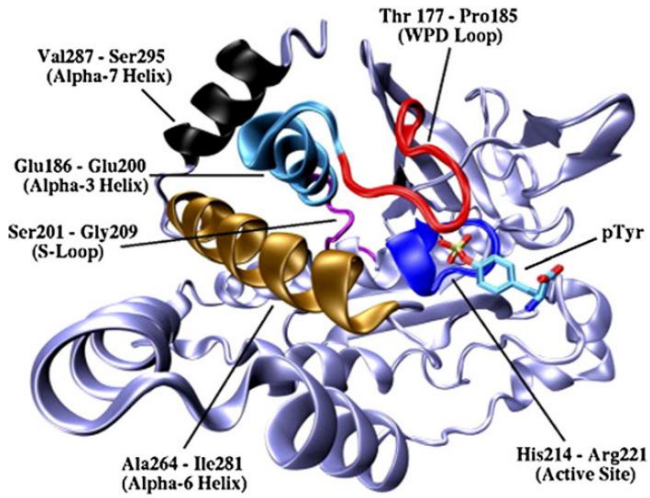

Fig. 2. Structural features of PTP1B as a ribbon diagram

PTP1B is located on the cytoplasmic face of the endoplasmic reticulum. The full length of PTP1B comprises 435 amino acids constituting the major cellular form, however, only a shorter length of 298 or 321 residues is typically considered for biochemical studies. As shown in Fig. 2, the active site of PTP1B consists of residues His214-Arg221 and loops WPD (Thr177-Pro185) and R (Val113-Ser118), which act as a gate upon ligand or substrate binding. Other important structural parts of PTP1B are S loop (Ser201-Gly209), α3-helix (Glu186-Glu200), α6-helix (Ala264-Ile281), and α7-helix (Val287-Ser295) that take part in catalysis. Crystallographic studies have shown that PTP1B exists in two forms, open and closed, i.e., unliganded and liganded PTP1B, respectively. The active site residues are accessible to substrate/ligand in the open form, but upon binding, conformational changes take place in the WPD, R, and S loops resulting in the closed form of the PTP1B.[21, 22] Closing of the WPD loop over substrate is an important event as it brings Asp181 into a favorable position relative to

ester oxygen of phosphotyrosine (pTyr). It enables Asp181 to act as a general acid and base catalyst in the two step process of dephosphorylation.[23, 24]

Mounting evidence from biochemical, genetic and pharmacological studies support a role for PTP1B as a negative regulator in multiple signaling pathways (Fig. 3), through the dephosphorylation of a variety of growth factor receptors, including the EGFR, PDGFR, IR, and IGF-IR, as well as cytosolic tyrosine kinases such as Src, p210Bcr-Abl, JAK2, TYK2, and STAT5, associating PTP1B with oncogenic, metabolic, and cytokine signaling.[25]

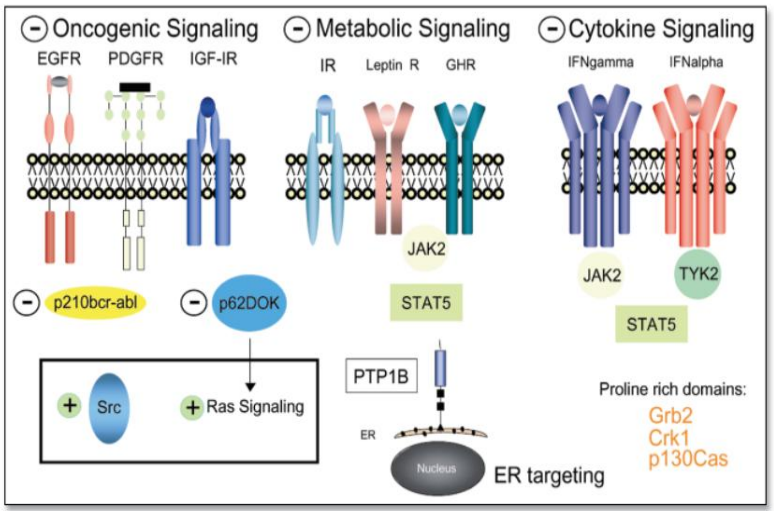

Fig. 3. PTP1B as a negative regulator of multiple signaling pathways

PTP1B has long been known to play a major role in inhibiting signaling from the insulin and leptin receptors. In the case of insulin signaling, PTP1B can associate with and dephosphorylate activated insulin receptor (IR) or insulin receptor substrates (IRS).[26] Overexpression of PTP1B in cell cultures decreases insulin-stimulated phosphorylation of IR and/or IRS-1, whereas reduction in the level of PTP1B, by antisense oligonucleotides or neutralizing antibodies, augments insulin-initiated signaling.[27, 28] PTP1B knockout mice display enhanced sensitivity to insulin, with increased or prolonged tyrosine phosphorylation of

IR in muscle and liver.[29] Interestingly, PTP1B knockout mice appears healthy, shows increased insulin sensitivity and enhanced glucose tolerance, and is resistant to weight gain on a high-fat diet. In the leptin pathway, PTP1B was subsequently shown to bind and dephosphorylate JAK2 (Janus kinase 2), which is downstream of leptin receptor.[30] Thus, the resistance to diet-induced obesity observed in $PTP1B^{-/-}$ mice is likely to be associated with increased energy expenditure owing to enhanced leptin sensitivity. Recent tissue-specific knockout results indicate that body weight, adiposity and leptin action can be regulated by neuronal PTP1B.[31] However, hints that PTP1B might also play a positive signaling role in cell proliferation began to emerge a few years ago, with the finding by a number of groups that PTP1B dephosphorylates the inhibitory Y529 site in Src, thereby activating this kinase.[32] Other PTP1B substrates might also contributes to pro-growth effects. Indeed, the idea that PTP1B can serve as a signaling stimulant in some cases received key confirmation in two landmark papers that showed PTP1B plays a positive role in a mouse model of ErbB2-induced breast cancer.[33, 34] Collectively, these studies provide strong proof-of-concept, validating the notion that inhibition of PTP1B could attract particular attention as a potential therapeutic target in obesity, diabetes, and now, cancer.

1.3. PTP1B role in breast cancer

Beyond the metabolic functions, recently, PTP1B has received renewed attention as an unexpected positive factor in ErbB2 induced breast tumorigenesis.[35] However, about 15-20% of human breast cancers display amplified and over-expressed ErbB2 (HER2, Neu), which is a receptor tyrosine kinase. ErbB2 overexpression is an adverse prognostic feature in early-stage breast cancer, associated with high tumor grade, increased tumor size, and increased nodal metastases.[36]

Tyrosyl phosphorylation is a reversible reaction, which is governed not only by PTKs, such as ErbB2, but also by PTPs. PTPs comprise a large super family and yet now little is known about the roles of specific PTPs in the normal mammary gland or in breast carcinogenesis. The PTPN1 gene, encoding PTP1B, is located within 20q13, a region frequently amplified in ovarian and breast cancers and usually associated with a poor prognosis.[37] Previous immunocytochemical studies showed that PTP1B is overexpressed in a significant subset (72%) of human breast[38] and ovarian[39] tumors and noted a correlation between PTP1B and HER2/Neu overexpression.[38] Furthermore, PTP1B expression reportedly is elevated in HER2/Neu-transformed human breast epithelial cells and tumors derived from such cells.[40] When transgenic mice over-expressing an activated form of ErbB2 (Neu) were crossed with a PTP1B knockout mice, the onset of ErbB2 (Neu)-driven breast cancer was delayed significantly in the absence of PTP1B, whereas transgenic PTP1B over-expression was sufficient to induce breast tumors in the absence of exogenous ErbB2.[33] Thus, PTP1B inhibitors may not only be useful in treatment of diabetes, obesity and metabolic syndrome, but ultimately offer a new treatment for breast cancer.

1.4. Plant triterpenoids

Triterpenoids are metabolites of isopentenyl pyrophosphate oligomers and represent the largest group of phytochemicals. It has been estimated that more than 20,000 triterpenoids exist in nature.[41] They predominantly are found in various plants including sea-weeds as well as in wax-like coatings of various fruits and medicinal herbs, including apples, cranberries, figs, olives, mistletoe, lavender, oregano, rosemary and thyme. Triterpenoids are biosynthesized in plants by the cyclization of squalene, a triterpene hydrocarbon and precursor of all steroids.[42] They can further be sub-classified into diverse groups including oleananes,

cucurbitanes, cycloartanes, dammaranes, euphanes, friedelanes, holostanes, hopanes, isomalabaricanes, lanostanes, limonoids, lupanes, protostanes, sqalenes, tirucallanes, ursanes and miscellaneous compounds.[43] Although triterpenoids were considered to be biologically inactive for a long period of time, accumulating evidence on their broad spectrum pharmacological activities coupled with a low toxicity profile has sparked renewed interest with regard to human health and disease. Triterpenoids are used for medicinal purposes in many Asian countries for antiinflammatory, analgesic, antipyretic, hepatoprotective, cardiotonic, sedative and tonic effects.[44] Recent studies have not only confirmed some of the aforementioned pharmacological properties of several triterpenoids, but also identified a variety of additional biological activities including anticarcinogenic activity.[45] An increasing number of triterpenoids have been reported to exhibit cytotoxicity against a variety of cancer cells without manifesting any toxicity in normal cells.[46] They also demonstrate antitumor efficacy in preclinical animal models of cancer.[43]

1.5. Triterpenoids and breast cancer

Breast cancer remains a major cause of death all over the world. There is still no effective cure for the vast majority of patients with advanced stages of breast cancer. These necessitate the search for novel preventive and therapeutic approaches. However, triterpenes from plants have long been studied in breast cancer and other types of cancer as well.[45] Among triterpenes, oleananes, cucurbitanes, ursanes and lupanes (Fig. 4) as well as other types of triterpenes have been reported to possess therapeutic potential in breast cancer treatment.

In 1999, three new oleanane-type triterpenes, namely remangilones A, B and C, were isolated from the dried leaves of *Physena madagascariensis*. Remangilones A and C have been found to be cytotoxic against MBA-MD-231 and MDAMB-435 cells.[47] Oleanolic acid, a well-

known triterpenes isolated from *Glossogyne tenuifolia*, has been reported to possess cytotoxicity against MCF-7 and MDA-MB-231 cells.[48] Furthermore, camellenodiol, camelledionol and other oleananes from *Camellia japonica* have been also reported to possess cytotoxicity against MCF7 cell lines.[45]

Ursolic acid, an ursane-type pentacyclic triterpenes have been acted as a potent inhibitor of MCF7 cell proliferation, exerting an early cytostatic response at G_1 phase of cell cycle followed by cell death.[49] Neto *et al.*[50] have isolated ursolic acid, promolic acid and related compounds from the bark and stem extract of *Polylepis racemosa* and all these natural products elicited cytotoxicity in MCF7 cell lines. Furthermore, bioactivity guided fractionation of the cranberry fruit has led to the identification of ursolic acid and novel ursolic acid esters with antitumor activities against MCF7 cells.[51]

A lupane type triterpene, betulinic acid has been isolated from the bark extract of *Syncarpia glomulifera* has shown antiproliferative activities toward MDA-MB-231 cells.[52] Betulinic acid also exhibited a remarkable cytotoxic effect against T47D cells with a simultaneous induction of apoptosis, decrease of *Bcl-2* and *cyclin D1* and increase of *Bax* gene expression. Moreover, in a recent study, betulin, which is also a lupine, has been found to inhibit the proliferation of T47D breast carcinoma cells.[53] Another well known lupane-type triterpene, lupeol has caused significant inhibition of growth of MDA-MB-231 cells in a dose-responsive manner. Interestingly, it has also been able to induce ERα expression in this ERα-negative breast cancer cell line.[54]

Cucurbitacins, originally isolated from several plants of the Cucurbitaceae family which possess medicinal properties, represent a group of diverse triterpenoids containing a cucurbitane skeleton. Cucurbitacin I has been found to inhibit the proliferation of MDA-MB-468 human breast cancer cells that express constitutively activated STAT3.[55] It also reduced

the levels of phosphotyrosine of constitutively activated STAT3 and induced apoptosis in the same tumor model. A new cucurbitacin D analog, 2-deoxycucurbitacin D as well as cucurbitacin D and 25-acetylcucurbitacin F have been isolated from the leaves of *Sloanea zuliaensis*. All these compounds have exhibited potent cytotoxic activity against MCF-7 human breast cancer cells.[56] Bioassay-guided purification of the fruit extract of *Cucurbita andreana* yielded cucurbitacin B, D, E and I and also reported for antitumor effects against MCF7 cell lines.[57]

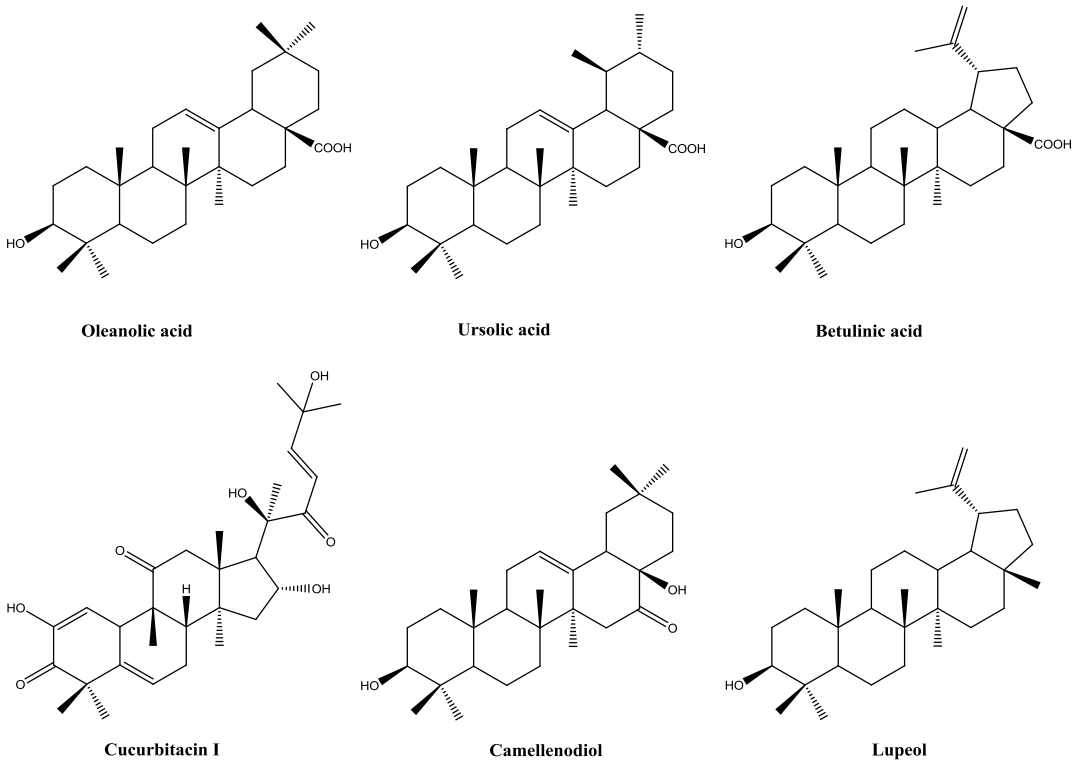

Fig. 4. Triterpenes with therapeutic potential in breast cancer

1.6. *Camellia japonica* L. (Theaceae)

Camellia japonica L. (English name ‘camellia’; Korean name ‘*dongbaek-kkot*’), an evergreen broad-leaved woody species from Theaceae family (Fig. 5), is cultivated as an ornamental or garden tree all over the Korea. It is widely distributed ranging from the southern and western coast of the Korean Peninsula through Taiwan, Kyushu and Shikoku to Honshu of Japan.[58]

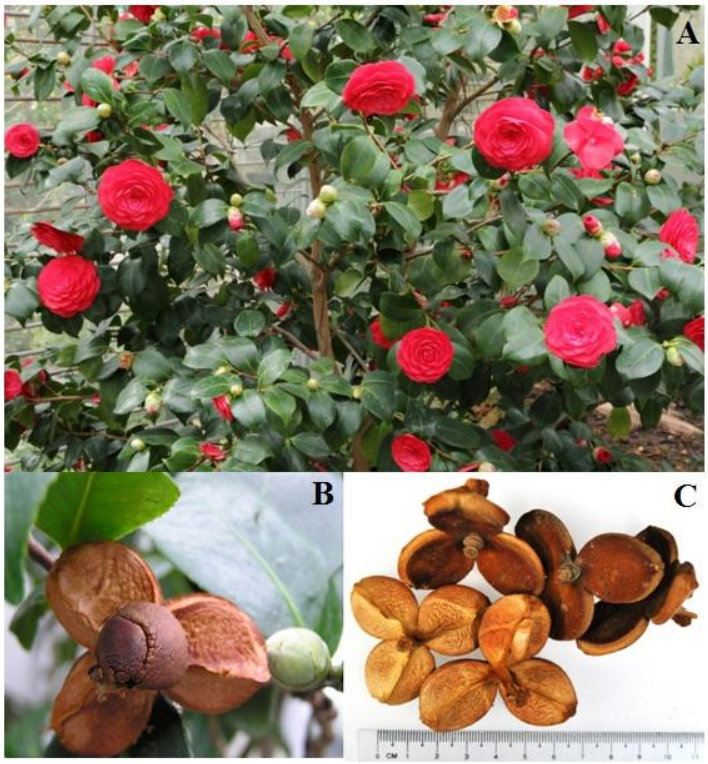

Fig. 5. *Camellia japonica* L. (A) Flower; (B) Fruit; (C) Fruit peel

The seeds of *C. japonica* have been used as a stomachic and antiinflammatory in Chinese folk medicine and also as an oil material,[59] while the flower buds have been used for the treatment of blood stagnation, vomiting blood and bleeding due to internal and external

injury, and also as an antiinflammatory, tonic, and stomachic in Japanese folk medicine and Chinese traditional medicine.[59, 60]

Extensive studies have been made on the constituents of different plant parts of *C. japonica* and a number of compounds have been reported including saponins in fruits[61-63] and seeds,[59, 64] flavonol glycosides in leaves,[65] hydrolyzable tannins,[66] acylated anthocyanins,[67] triterpenes[68] and purin alkaloids[69] in flowers and triterpenes in seed oil.[70]

Regarding the bioactive constituents in leaves, flavonol glycosides having antioxidant activity,[65] triterpenes having cytotoxic activity,[45] and saponins having anti-fungal or antifeedant activity toward yellow butterfly larvae,[71] gastro protective and platelet aggregation activity[60] have been reported. Furthermore, some tannins from leaves, flower buds, and fruits have been shown to have an inhibitory effect on human immunodeficiency virus-1 (HIV-1) protease.[72-74]

However, according to literature studies, chemical constituents from fruit peels of *C. japonica* have not been reported yet. Moreover, although plant triterpenes have long been studied and reported for strong PTP1B inhibitory activity as well as therapeutic potential in breast cancer, but there is no study on camellia triterpenes with PTP1B inhibitory activity and related cytotoxicity against breast cancer cell lines. In this study, bioactivity guided fractionation of an EtOAc-soluble extract of fruit peels of *C. japonica* resulted in the isolation of six new (**1**-**6**), along with eight known (**7**-**14**) oleanane-type triterpenes. Among all, four new 3, 4-*seco*-oleanane-type triterpenes (**3-6)** are reported for the first time not only from *C. japonica* but also from Camellia genus. All the isolates were evaluated for their inhibitory effects on PTP1B enzyme, as well as their growth inhibition on MCF7, adriamycin-resistant MCF7 (MCF7/ADR) and MDA-MB-231 breast cancer cell lines.

2. Materials and Methods

2.1. Materials

2.1.1. Plant material

The fruit peels of *C. japonica* was collected from Jeju Island, Korea in 2011 and botanically identified by Prof W. K. Oh. A voucher specimen (CU2011-01) has been deposited at the laboratory of natural products chemistry, College of pharmacy, Chosun University, Gwangju, Republic of Korea.

2.1.2. Chemicals, reagents and chromatography

Open column chromatography was conducted on silica gel (63-200 and 40-63 μm particle size) and RP-18 (40-63 μm particle size) from Merck. TLC was carried out with silica gel 60 F_{254} and RP-18 F_{254} plates from Merck. HPLC was carried out using a Gilson system with a UV detector and Optima Pak C_{18} column (10×250 mm, 10μm particle size, RS Tech, Korea). HPLC solvents MeOH and MeCN were purchased from B&J (Burdick & Jackson®, USA). Deuterated solvents $CDCl_3$ and acetone were purchased from CIL (Cambridge Isotope Lab., USA) for NMR analysis.

Ursolic acid, tamoxifen and MTT [3-(4, 5-dimethylthiazol-2-yl)-2, 5-diphenyl-tetrazolium bromide] were purchased from Sigma-Aldrich (St Louis, MO, USA). PTP1B (human, recombinant) was purchased from BIOMOL International LP (USA). Dulbecco's modified eagle's medium (DMEM), fetal bovine serum (FBS), and trypsin were purchased from GIBCO-BRL (Grand Island, NY, USA).

2.1.3. General experimental procedures

Optical rotations were determined on a Rudolph Autopol IV polarimeter using a 100 mm glass microcell. IR spectra (KBr) were recorded on a Nicolet 6700 FT-IR (Thermo Electron Corp.). The 1D and 2D NMR spectra (^{1}H and ^{13}C NMR, NOESY, HSQC and HMBC) were performed using a Varian Unity Inova 500 MHz spectrometer with TMS as the internal standard. HR-EIMS data were recorded on a Micromass QTOF2 spectrometer. HR-FABMS data were obtained with JEOL JMS-700 mass spectrometer. Silica gel (Merck, 63-200μm and 40-63 μm particle size), RP-18 (Merck, 40−63μm particle size) were used for column chromatography. TLC was carried out with silica gel 60 F_{254} and RP-18 F_{254} plates. HPLC was carried out using Gilson HPLC system with 321 pump and UV/VIS-155 detector. Optima Pak C_{18} column (10×250 mm, 10μm particle size, RS Tech, Korea) was used as HPLC column. All solvents used for extraction and isolation were of analytical grade.

2.2. Methods

2.2.1. Extraction and isolation

The dried fruit peels of *Camellia japonica* (7 kg) were extracted with MeOH (10 L x 3 times) at room temperature for one week. The combined MeOH extracts were concentrated to yield a dry residue (220.0 g). This crude extract was then suspended in H_2O (2 L) and partitioned successively with *n*-hexane (3 ×2 L), EtOAc (3×2 L), and *n*-BuOH (3×2 L). The EtOAc fraction (50.0 g), which exhibited both PTP1B inhibitory and cytotoxic activity (>50% inhibition at 30 μg/mL) was chromatographed over a silica gel column (15x30 cm; 63−200μm particle size) and eluted with a gradient mixtures of *n*-hexane/acetone (9:1, 8:2, …., 1:9, each 2 L) to yield five pooled fractions (F1: 3.8 g; F2: 4.1 g; F3: 3.5 g; F4: 18.2 g; F5: 5.6 g). Fraction

F2 was further applied to silica gel column (5x30 cm; 40-63µm particle size) and eluted with a gradient mixture of *n*-hexane/EtOAc (10:1, 8:1…., 2:1) to afford five subfractions (F2.1-F2.5). F2.3 (350 mg) was purified by HPLC [Optima Pak C_{18} column (10 ×250 mm, 10µm particle size, RS Tech, Korea); mobile phase MeOH in H_2O containing 0.1% HCO_2H (0-25 min: 90% MeOH, 25-27 min: 90-95% MeOH, 27-50 min: 95% MeOH, 50-52 min: 95-100% MeOH, 52-60 min: 100% MeOH); flow rate 2 mL/min; UV detection at 205 and 254 nm] to yield compounds **7** (t_R = 21 min, 101 mg), **8** (t_R = 31 min, 3.5 mg), **1** (t_R = 33 min, 7.1 mg), **9** (t_R = 45 min, 16.5 mg) and **10** (t_R = 47 min, 68 mg). Fraction F3 was chromatographed over a silica gel column (5x30 cm; 40-63µm particle size) and eluted with a gradient mixture of CH_2Cl_2/MeOH (50:1, 45:1, 40:1….., 5:1) to afford six subfractions (F3.1-F3.6). F.3.4 (200 mg) was purified by HPLC (0-35 min: 83% MeOH, 35-37 min: 83-100% MeOH, 37-45 min: 100% MeOH) to yield compound **11** (t_R = 30 min, 110 mg). Furthermore, F3.5 (600 mg) was fractionated into five subfractions (F3.5.1-F3.5.5), using a RP-18 column (4x30 cm; 40-63µm particle size), with a stepwise gradient of MeOH/H_2O (1:1 to 10:1). Subfraction F3.5.2 (70.8 mg) was purified by HPLC (0−40 min: 80% MeOH, 42−44 min: 80-100% MeOH, 44-52 min: 100% MeOH) to yield compound **2** (t_R = 35 min, 15 mg). Moreover, subfraction F3.5.3 (65.2 mg) was purified by HPLC (0-35 min: 88% MeOH, 35-37 min: 88-100% MeOH, 37-45 min: 100% MeOH) to yield compound **12** (t_R = 30 min, 10.2 mg). Similarly, compounds **13** (t_R = 40 min, 4.5 mg) and **14** (t_R = 45 min, 33 mg) were purified by HPLC (0-50 min: 88% MeOH, 50-52 min: 88-100% MeOH, 52-60 min: 100% MeOH) from subfraction F3.5.4 (120 mg). Fraction F4 was applied to RP-18 column (8x30 cm; 40-63µm particle size), with a stepwise gradient of MeOH/H_2O (1:1 to 10:1) to yield seven subfractions (F4.1-F4.7). Next, F4.6 (4.1 g) was further fractionated into five subfractions (F4.6.1-F4.6.5), by using a silica gel column (5x30 cm; 40-63µm particle size); eluted with a gradient mixture of CH_2Cl_2/MeOH (40:1, 35:1,

30:1….., 1:1). Then, subfraction F4.6.3 (1.1 g) was chromatographed over a silica gel column (4x30 cm; 40-63μm particle size) and eluted with a gradient mixtures of *n*-hexane/acetone (8:1, 7:1, …., 1:1) to obtain four subfracions (F4.6.3.1- F4.6.3.4). F4.6.3.1 (65 mg) was purified by HPLC (0-50 min: 46% MeCN, 50-52 min: 46-100% MeCN, 52-60 min: 100% MeCN) to yield compound **6** (t_R = 47 min, 11.8 mg). Furthermore, F4.6.3.2 (150 mg) was purified by HPLC (0-50 min: 42% MeCN, 50-52 min: 42-100% MeCN, 52-60 min: 100% MeCN) to yield compounds **3** (t_R = 25 min, 15.6 mg) and **5** (t_R = 42 min, 18.5 mg). On the other hand, subfraction F4.6.4 (1 g) was chromatographed over a silica gel column (4x30 cm; 40-63μm particle size) and eluted with a gradient mixtures of *n*-hexane/acetone (5:1, 4:1, …., 1:1) to obtain four subfracions (F4.6.4.1- F4.6.4.4). Finally, F4.6.4.1 (150 mg) was purified by HPLC (0-45 min: 48% MeCN, 45-47 min: 48-100% MeCN, 47−55 min: 100% MeCN) to yield compound **4** (t_R = 42 min, 30 mg).

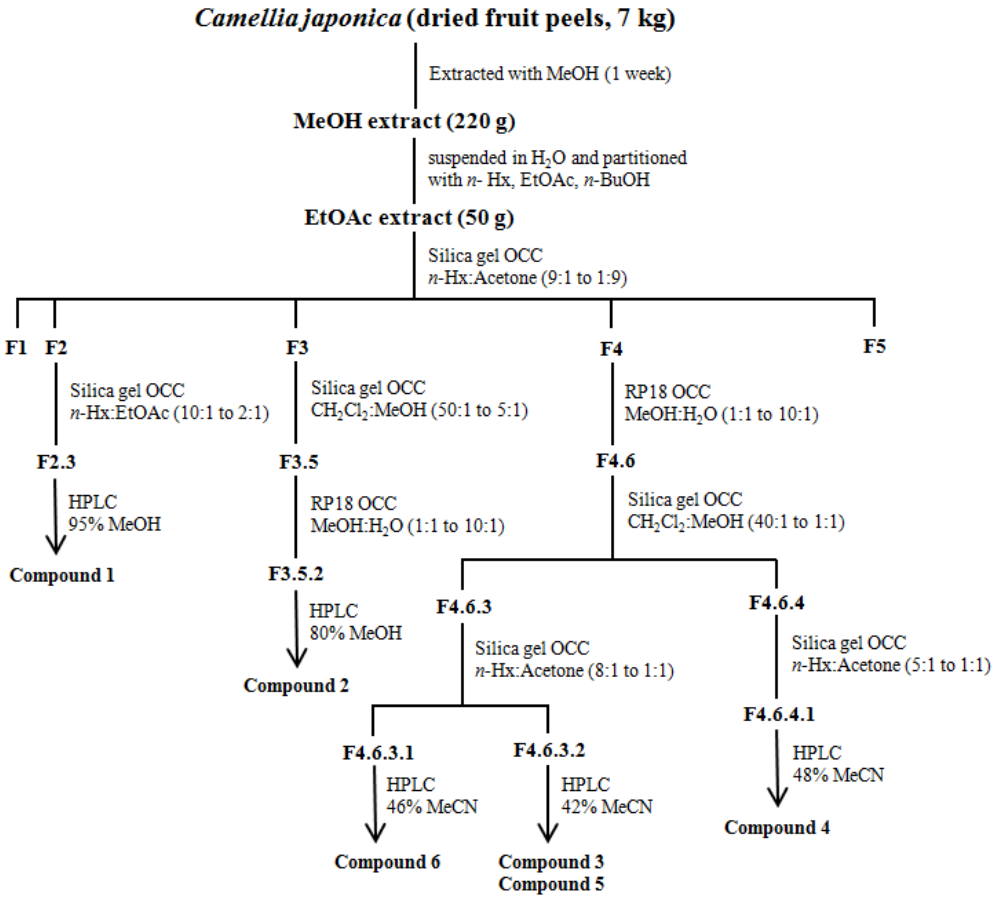

Scheme 1. Isolation of new compounds (**1**–**6**) from *C. japonica*

3, 16-dioxo-olean-12(13), 17(18)-diene (1)

Brown, amorphous powder; $[\alpha]_D^{25}$ +28.9 (*c* 0.1, $CHCl_3$); IR (KBr) ν_{max} 2952, 2869, 1705, 1665 cm^{-1}; ^1H (500 MHz) and ^{13}C (125 MHz) NMR data, see Table 1; HR-EIMS *m/z* 422.3187 $[M]^+$ (calcd for $C_{29}H_{42}O_2$, 422.3185).

3β, 16α, 17 –trihydroxy- olean-12-ene (2)

White, amorphous powder; $[\alpha]_D^{25}$ +32.7 (c 0.1, $CHCl_3$); IR (KBr) v_{max} 3615, 3431, 2937, 1652 cm^{-1}; ^1H (500 MHz) and ^{13}C (125 MHz) NMR data, see Table 2; HR-EIMS, m/z 444.3605 $[M]^+$ (calcd for $C_{29}H_{48}O_3$, 444.3603).

Camelliaolean A (3)

Brown, amorphous powder; $[\alpha]_D^{25}$ +26.8 (*c* 0.1, $CHCl_3$); IR (KBr) ν_{max} 3374, 2863, 1740, 1710, 1623 cm^{-1}; ^1H (500 MHz), ^{13}C (125 MHz) NMR data, see Table 3; HR-FABMS (*m/z* 541.3517 $[M + Na]^+$, calcd 541.3505).

Camelliaolean B (4)

White, amorphous powder; $[\alpha]_D^{25}$ +35.1 (*c* 0.1, $CHCl_3$); IR (KBr) ν_{max} 3363, 2951, 1742, 1713, 1459 cm^{-1}; ^1H (500 MHz), ^{13}C (125 MHz) NMR data, see Table 4; HR-FABMS (*m/z* 527.3350 $[M + Na]^+$, calcd 527.3349).

Camelliaolean C (5)

White, amorphous powder; $[\alpha]_D^{25}$ +24.7 (*c* 0.1, $CHCl_3$); IR (KBr) ν_{max} 3370, 2867, 1735, 1713, 1628 cm^{-1}; ^1H (500 MHz), ^{13}C (125 MHz) NMR data, see Table 5; HR-FABMS (*m/z* 525.3188 $[M + Na]^+$, calcd 525.3192).

Camelliaolean D (6)

Brown, amorphous powder; $[\alpha]_D^{25}$ +28.3 (*c* 0.1, $CHCl_3$); IR (KBr) ν_{max} 3360, 2872, 1730, 1710, 1615 cm^{-1}; ^1H (600 MHz), ^{13}C (150 MHz) NMR data, see Table 6; HR-FABMS (*m/z* 473.3283 $[M + H]^+$, calcd 473.3267).

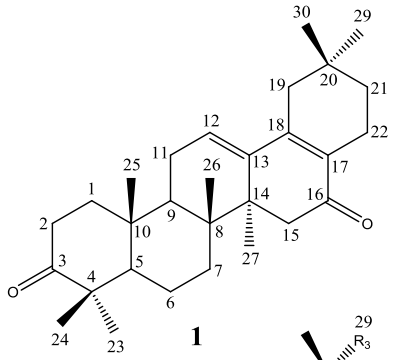

1

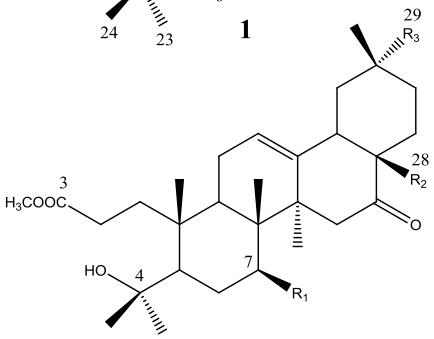

	R_1	R_2	R_3
3	H	CH_2OH	CH_2OH
4	β-OH	OH	CH_3

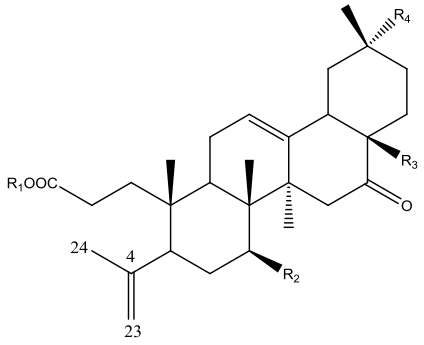

	R_1	R_2	R_3	R_4
5	CH_3	β-OH	OH	CH_2OH
6	H	H	OH	CH_2OH

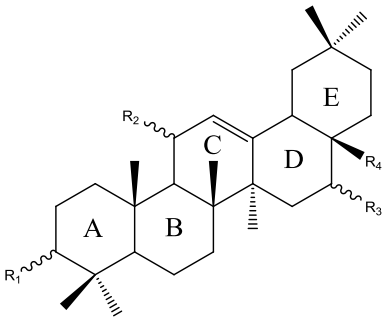

	R_1	R_2	R_3	R_4
2	β-OH	H	α-OH	OH
7	=O	H	=O	OH
10	β-OAc	H	H	COOH
11	β-OH	H	=O	OH
12	β-OAc	=O	H	CH_3
14	β-OH	H	H	COOH

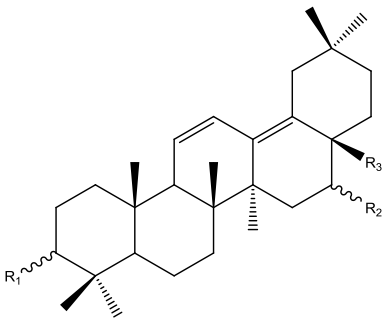

	R_1	R_2	R_3
8	β-OH	H	COOH
9	β-OAc	H	COOH
13	β-OH	=O	H

Fig. 6. Chemical structures of compounds **1-14** isolated from *Camellia japonica*

2.2.2. PTP1B inhibition assay

PTP1B (human, recombinant) was purchased from BIOMOL International LP (USA) and the enzyme activity was measured using *p*-nitrophenyl phosphate (*p*-NPP) as a substrate.[75] To each of 96-wells (final volume: 100µL), 4 mM *p*-NPP and PTP1B (0.05–0.1µg) in a buffer containing 50 mM citrate (pH 6.0), 0.1 M NaCl, 1 mM EDTA, and 1 mM dithiothreitol (DTT) were added with or without test compounds. Following incubation at 37°C for 30 min, the reaction was terminated with 10 N NaOH. The amount of produced *p*-nitrophenol was estimated by measuring the absorbance at 405 nm. The nonenzymatic hydrolysis of 4 mM *p*-NPP was corrected by measuring the increase in absorbance at 405 nm obtained in the absence of PTP1B enzyme.

2.2.3. Kinetic parameters for PTP1B inhibition type

To determine the inhibition type, two kinetic methods namely Lineweaver-Burk and Dixon plots were used.[76, 77] Using Lineweaver-Burk double reciprocal plots, the PTP1B inhibition mode was determined at various concentrations of *p*-NPP substrate (1, 2, 4, 8, and 16 mM) in the absence or presence of different test compound concentrations (0, 2, 4 and 8 µM). Each enzymatic inhibition of test compounds was evaluated by monitoring the effects of different concentrations of the substrates in the Dixon plots (single reciprocal plot). The inhibition constant (K_i) values were determined by interpretation of the Dixon plots.

2.2.4. Cell culture

The screening cell lines (MCF7 and MDA-MB-231 human breast carcinoma cells, and the adriamycin resistant cell line MCF7/ADR) were maintained at 37°C in a humidified

atmosphere containing 5% CO_2. All the media used were DMEM supplemented with 10% heat-inactivated fetal bovine serum, 4.5 g/L D-glucose, 100 mg/L sodium pyruvate and L-glutamine. The cells were sub cultured every 3 days using the standard trypsinization procedure.

2.2.5. MTT cytotoxicity assay

The cell viability was assessed using a MTT based cytotoxicity assay[78] to determine the IC_{50} of the isolated compounds. In these assays, $1x10^4$ MCF7 (ER positive weakly invasive), MDA-MB-231 (ER negative highly invasive), and MCF7/ADR (adriamycin resistant) cells in 100 µL of the culture medium per well were seeded in 96-well plates and allowed to adhere for 24 h prior to treatment. At various concentrations, the cells in 96 well plates were treated and incubated for 48 h. The final concentration of DMSO in the culture medium was maintained at 0.05% (v/v) to avoid solvent toxicity. Subsequently, 20 µL of the 2 mg/mL MTT solution was added to each well of the plate and incubated 4 h. Then the absorbance was measured at 550 nm. The percentage cell viability is expressed as toxicities of the compounds, where the higher the toxicity, the lower the cell viability. Percentage cell viability is defined as the absorbance in the experiment well compared to that in the control wells. The cytotoxicity results are expressed as the mean ± SD and represent the concentration inhibiting 50% cell growth (IC_{50}). Each experiment was carried out in triplicates.

2.2.6. Statistical analysis

The results were expressed as mean ± standard deviation (SD) from triplicate experiments and evaluated by using SigmaPlot® (version 11.0) software.

3. Results and Discussions

3.1. Structural determination of new compounds 1-6

Bioassay-guided fractionation of an EtOAc soluble extract of fruit peels of *Camellia japonica* led to the isolation of a series of oleanane-type triterpenes, consisting of two new oleanane (**1**-**2**) and four new *seco*-oleanane (**3**-**6**), along with eight known oleanane (**7**-**14**) type triterpenes (Fig. 6). The known compounds were identified as camelledionol (**7**),[68] 3β-hydroxy-olean-11,13(18)-diene-28-oic acid (**8**),[79] 3β-acetoxy-olean-11,13(18)-diene-28-oic acid (**9**),[80] 3β-acetoxy-olean-12-ene-28-oic acid (**10**),[81] camellenodiol (**11**),[60] 3β-acetoxy-11-oxo-olean-12-ene (**12**),[82] 3β-hydroxy-16-oxo-olean-11,13(18)-diene (**13**),[80, 83] and oleanolic acid (**14**)[84] on the basis of spectroscopic analysis, chemical evidence and comparison with spectral data with those reported in the literatures.

3.1.1. Structural determination of compound 1

Compound **1** was obtained as a brown amorphous powder with positive optical rotation ($[\alpha]_D^{25}$ +28.9 in $CHCl_3$). The IR spectrum showed strong absorption band at 1665 cm^{-1} indicating the presence of α,β-unsaturated ketone group with extended conjugation. In addition, HREIMS spectrum of compound **1** exhibited a molecular ion peak at *m/z* 422.3187 $[M]^+$ (calcd 422.3185), corresponding to a molecular formula of $C_{29}H_{42}O_2$ with nine double-bond equivalents, of which five were accounted for by a pentacyclic ring system, two by two olefinic bonds, and two by two ketocarbonyl groups. The ^1H NMR spectrum (Table 1) showed signals for seven methyl groups [δ_H 0.92, 0.94, 0.99, 1.07, 1.09, 1.11, 1.12 (3H each, all s)] and an olefinic proton [δ_H 6.13 (1H, t, J= 4.0 Hz). The ^{13}C NMR spectrum (Table 1) revealed the

presence of four olefinic carbons at δ_C 126.54, 129.32, 139.47 and 146.94 and two α,β-unsaturated ketone groups at δ_C 200.31 and 217.56. These results were closely similar to those of maragenin II, which was also isolated and reported previously from this plant.[68] The most obvious distinction between compound **1** and maragenin II was the chemical shift value of C-3, which appeared as a ketone carbon at δ_C 217.56 for **1** instead of an oxymethine carbon at δ_C 78.7 for maragenin II. However, the attachment of one ketone group at C-3 was confirmed by HMBC correlation from H_2-1 (δ_H 1.96, 1.50) and H_2-2 (δ_H 2.55, 2.45); from H_3-23 (δ_H 1.11) and H_3-24 (δ_H 1.07) to ketone carbon at δ_C 217.56 (Fig. 7). Furthermore, HMBC correlation from H_2-15 (δ_H 2.62, 2.20), and H-22 (δ_H 2.20) to ketone carbon at δ_C 200.31 indicated the attachment of another ketone group at C-16 position. Therefore, from the spectroscopic data as well as comparison with the data from known compounds, **1** was identified as 3,16-dioxo-olean-12(13),17(18)-diene.

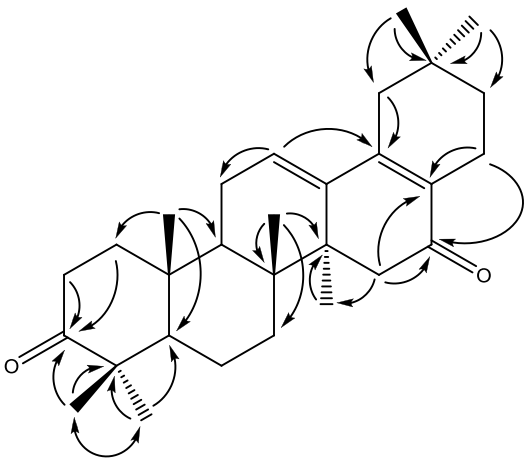

Fig. 7. Key HMBC (H→C) correlations of compound **1**

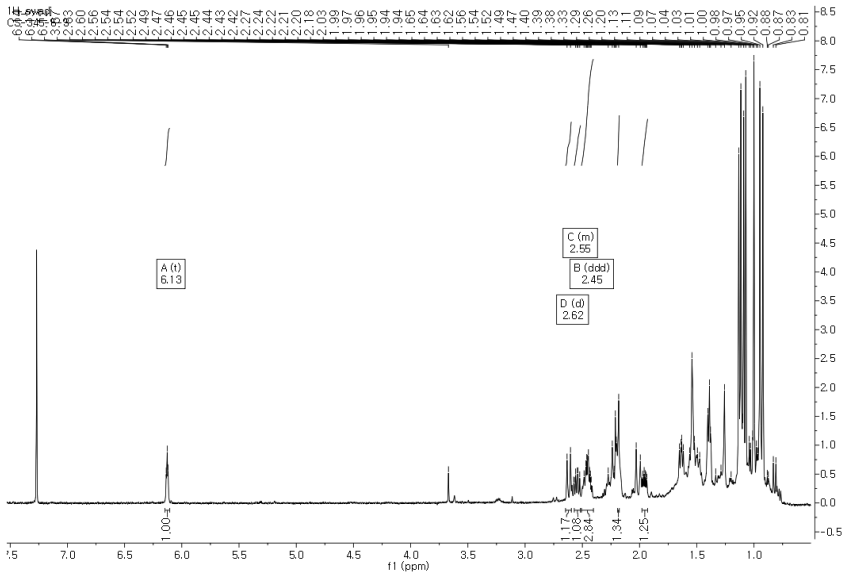

Fig. 8. ^{1}H-NMR ($CDCl_3$ 500 MHz) spectrum of compound **1**

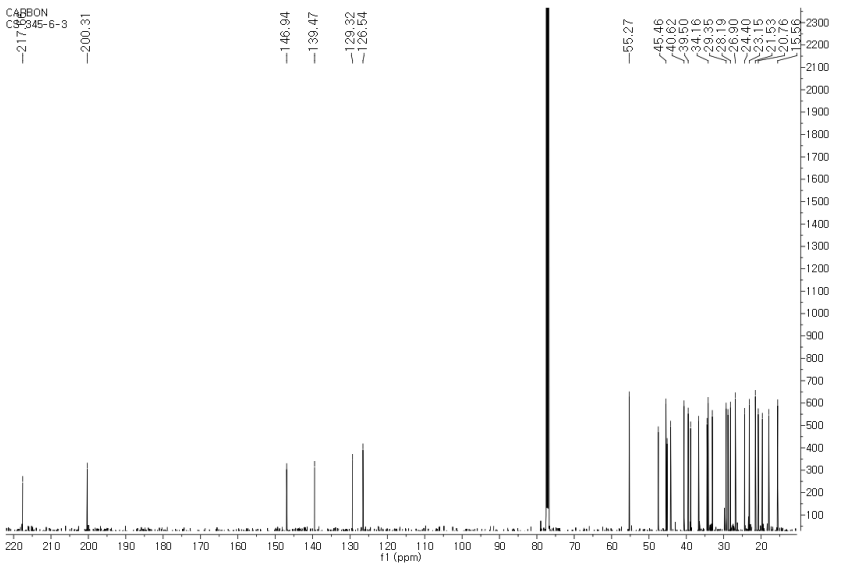

Fig. 9. ^{13}C-NMR ($CDCl_3$ 125 MHz) spectrum of compound **1**

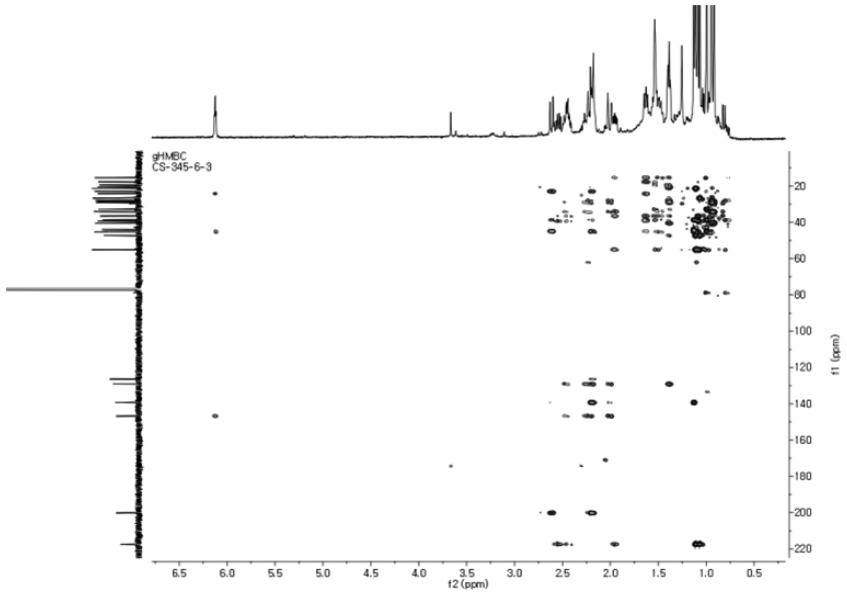

Fig. 10. HMBC spectrum of compound **1**

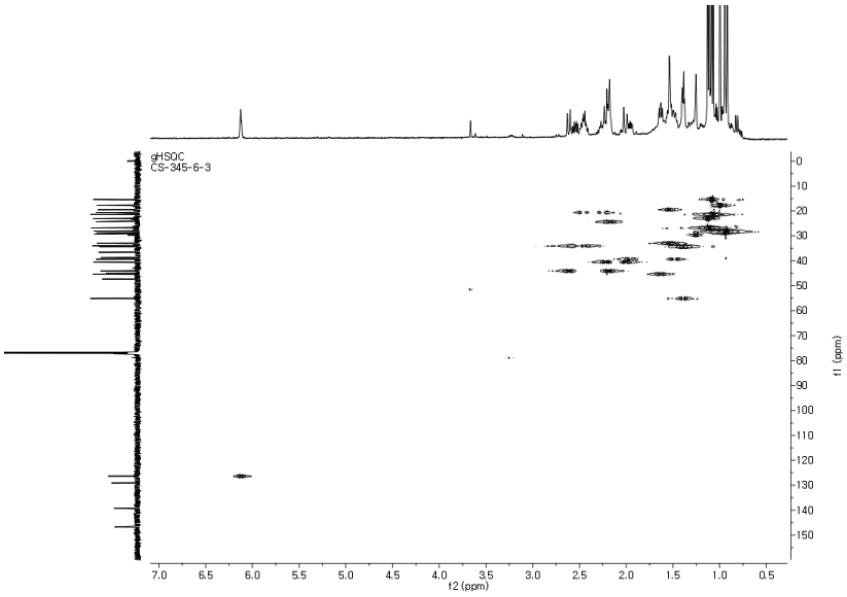

Fig. 11. HSQC spectrum of compound **1**

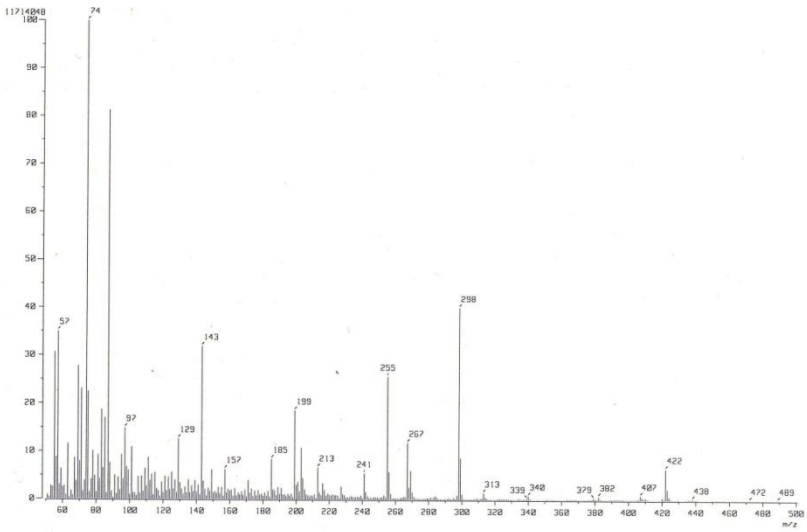

Fig. 12. EIMS spectrum of compound **1**

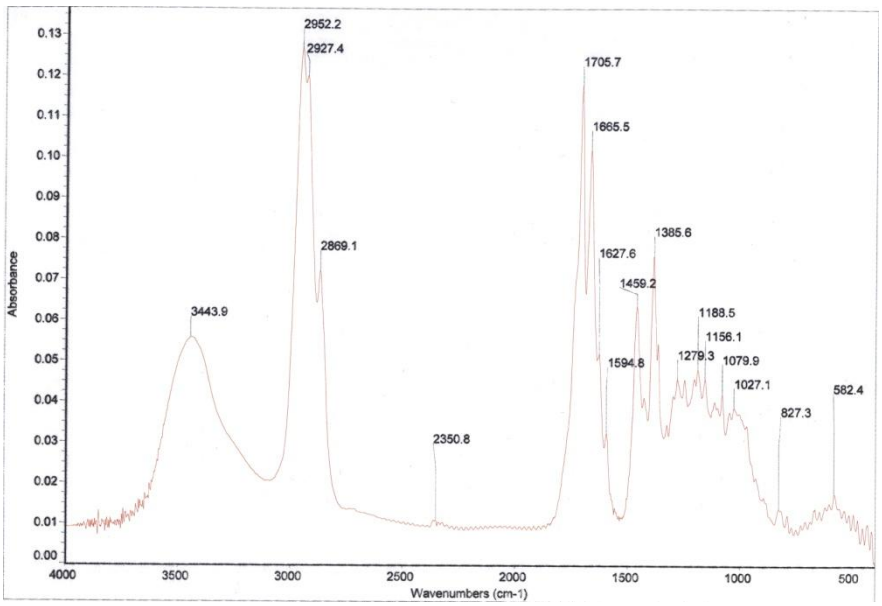

Fig. 13. IR (KBr) spectrum of compound **1**

Table 1. ^{1}H (500 MHz) and ^{13}C (125 MHz) -NMR data of compound **1**[a] in $CDCl_3$

Position	δ_H mult. (*J* in Hz)	δ_C	HMBC (H→C)
1	1.96 m	39.50	C-2, C-3, C-10
	1.50 m		
2	2.55 m	34.16	C-1, C-3, C-10
	2.45 m		
3		217.56	
4		47.50	
5	1.40 m	55.27	C-3, C-6, C-23, C-24, C-25
6	1.55 m	19.65	C-5, C-7, C-23
	1.55 m		
7	1.55 m	33.05	C-6, C-8, C-14, C-26
	1.55 m		
8		38.86	
9	1.63 dd (10.5, 7.0)	45.46	C-8, C-10, C-11, C-25, C-26
10		36.70	
11	2.18 m	24.40	C-9, C-12
12	6.13 t (4.0)	126.54	C-11, C-18
13		139.47	
14		45.14	
15	2.62 d (14.8)	44.19	C-14, C-16, C-17, C-27
	2.20 d (14.6)		
16		200.31	
17		129.32	
18		146.94	
19	2.18 m	40.62	C-18, C-20, C-29, C-30
	1.98 m		
20		29.35	
21	1.39 m	34.47	C-22, C-29, C-30
	1.39 m		
22	2.50 m	20.76	C-21, C-16, C-17
	2.20 m		
23	1.11 s	26.90	C-3, C-4, C-5, C-24
24	1.07 s	21.53	C-4, C-5, C-23
25	1.09 s	15.56	C-1, C-5, C-9, C-10
26	0.99 s	17.94	C-7, C-8, C-9, C-14
27	1.12 s	23.15	C-8, C-13, C-14, C-15
28			
29	0.94 s	28.86	C-19, C-20, C-21, C-30
30	0.92 s	28.19	C-19, C-20, C-21, C-29

[a] Assignments were based on HMBC, HSQC experiments

3.1.2. Structural determination of compound 2

Compound **2**, a white, amorphous powder, exhibited a positive optical rotation ($[\alpha]_D^{25}$ +32.7 in $CHCl_3$). Its IR spectrum showed absorption bands for hydroxy and trisubstituted double bond at ν_{max} 3431 and 1652 cm^{-1}, respectively. In addition, the molecular formula was determined as $C_{29}H_{48}O_3$ from a molecular ion peak at *m/z* 444.3605 $[M]^+$ (calcd for $C_{29}H_{48}O_3$: 444.3603) in the HREIMS spectrum. Moreover, The EIMS spectrum showed a typical fragment ion peak at *m/z* 236, which is the characteristic ion peak of retro-Diels-Alder fragmentation occurring in the C ring of a 12-oleanane-type triterpene, indicating that compound 2 belongs to an oleanane-type triterpene.[85] The ^1H NMR spectrum (Table 2) showed the presence of seven methyl groups [δ_H 0.79, 0.91, 0.91, 0.93, 1.00, 1.01, 1.37(3H each, all s)], two oxymethines [δ_H 3.23 (1H, dd, J= 3.9, 11.3 Hz), 3.91 (1H, s like)], and a characteristic olefinic proton [δ_H 5.40 (1H, s like)]. Furthermore, the ^{13}C NMR spectrum (Table 2) showed 29 carbon signals, including two olefinic carbons at δ_C 124.68 and 142.31, three oxygenated carbon at δ_C 71.63, 77.97, and 78.95, and seven tertiary methyl carbons at δ_C 15.43, 15.62, 17.23, 24.48, 26.84, 28.11, and 32.47. The other carbon signals were observed and assigned to nine methylenes, three methines and five quaternary carbons. The ^1H NMR data coupled with ^{13}C NMR data of compound **2** resembled with those of Camellioside E,[86] except for the hydroxy group substitution in ring A at C-3 position. These results were evidenced by characteristic peak at δ_H 3.23 (1H, dd, J= 11.3, 3.9 Hz) with corresponding ^{13}C NMR signal from HSQC at δ_C 78.95. These assignments were further confirmed from the HMBC correlations from H_2-2 (δ_H 1.64, 1.55) to C-3 (δ_C 78.95); from H-3 (δ_H 3.23) to C-23 (δ_C 28.11) and C-24 (δ_C 15.62); from H-5(δ_H 0.78) to C-3 (δ_C 78.95) (Fig. 14). The relative configuration of this hydroxy group at C-3 was determined as β due to the high coupling constant (J= 11.3, 3.9 Hz) and from NOE correlation between proton pair H-3α and H-5, H_3-23. HMBC

correlation from one relatively deshielded oxymethine proton signal at δ_H 3.91 to C-14 (δ_C 41.22), C-17 (δ_C 71.63) and C-18 (δ_C 47.94) as well as correlation from H_2-15 (δ_H 2.22, 1.25), and H_2-22 (δ_H 1.85, 1.73) to carbon signal at δ_C 77.97 inferred the presence of another hydroxy group at C-16 position. The broad singlet signal at H-16 (δ_H 3.91) indicated the α-orientation of this hydroxy group which was further supported in NOESY spectrum (Fig. 14) from the cross peaks between proton pairs H-15α and H-16, H_3-27; H-15β and H-16. Finally, the third hydroxy group was confirmed to be located at C-17 position on the basis of HMBC correlations from H_2-15 (δ_H 2.22, 1.25) to C-17 (δ_C 71.63); from H-18 (δ_H 2.36) to C-17 (δ_C 71.63); and from H_2-22 (δ_H 1.85, 1.73) to C-17 (δ_C 71.63). Therefore, the structure of compound **2** was elucidated as 3β,16α,17-trihydroxy-olean-12-ene.

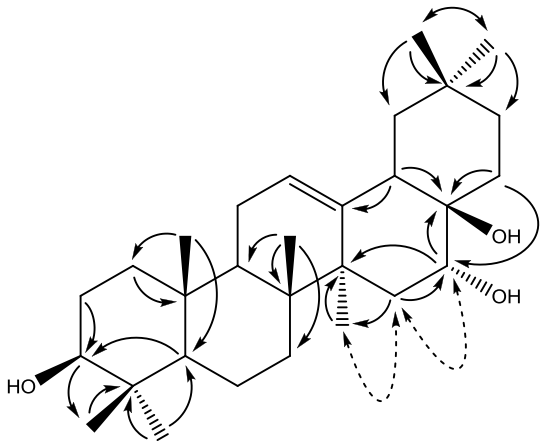

Fig. 14. Key HMBC (H→C) and NOESY (H⋯►H) correlations of compound **2**

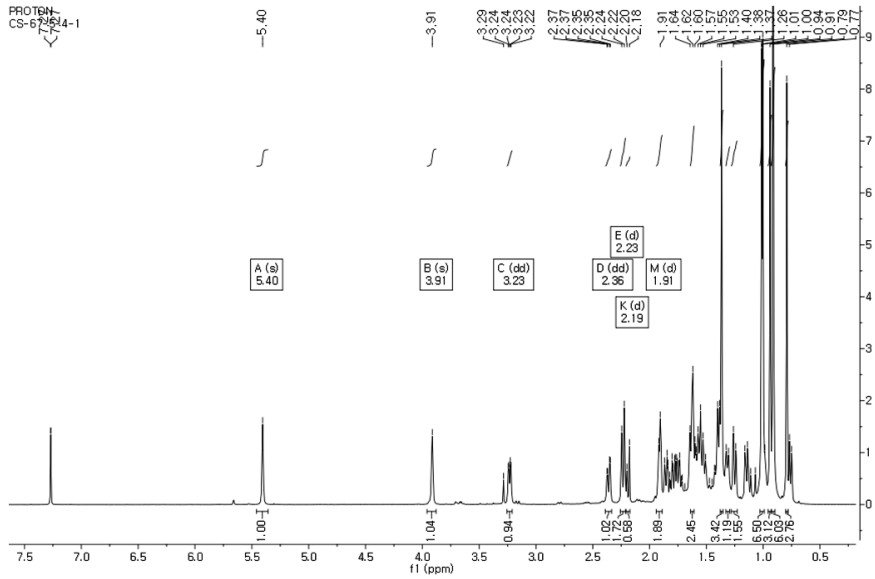

Fig. 15. ^{1}H-NMR ($CDCl_3$ 500 MHz) spectrum of compound **2**

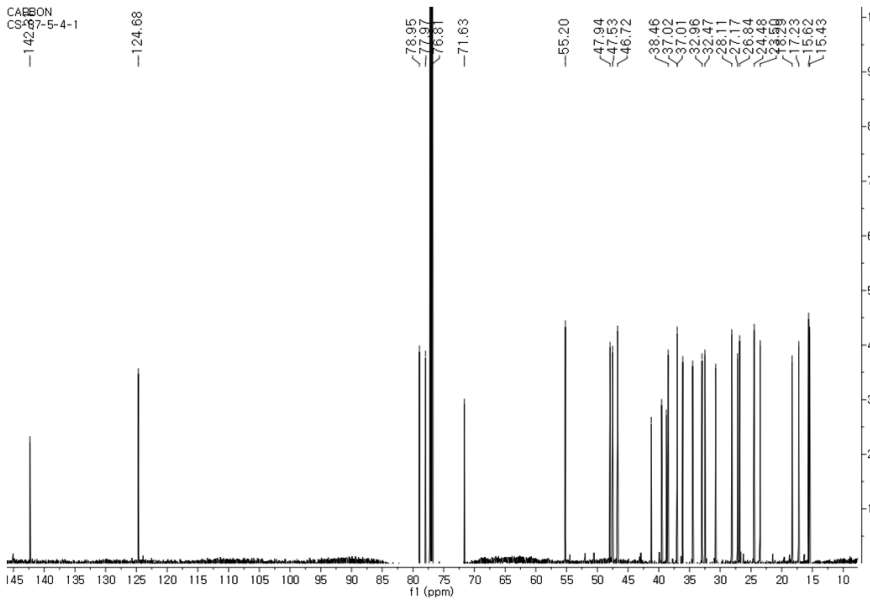

Fig. 16. ^{13}C-NMR ($CDCl_3$ 125 MHz) spectrum of compound **2**

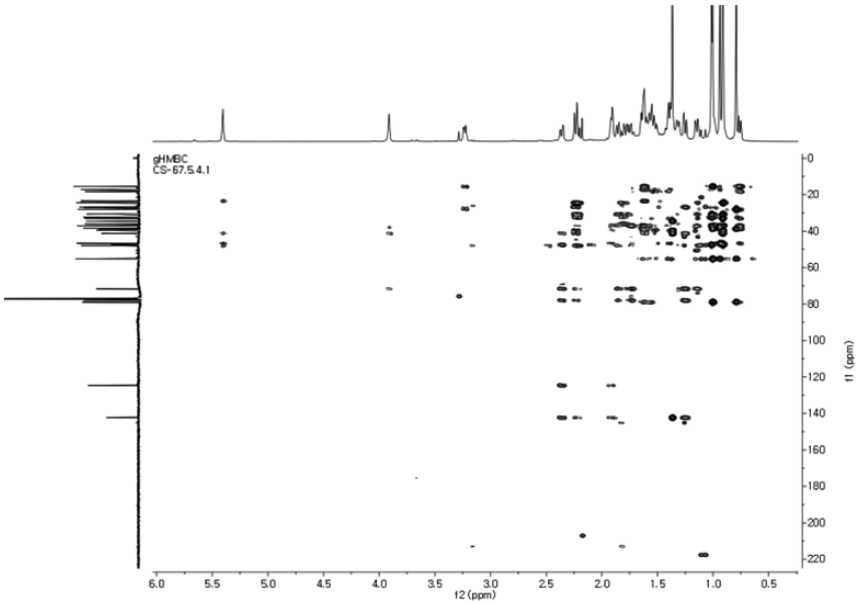

Fig. 17. HMBC spectrum of compound **2**

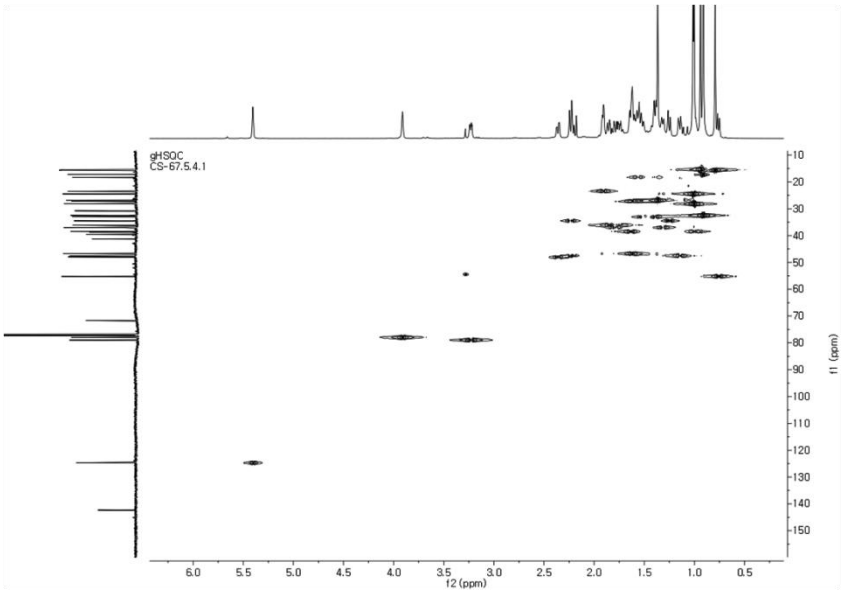

Fig. 18. HSQC spectrum of compound **2**

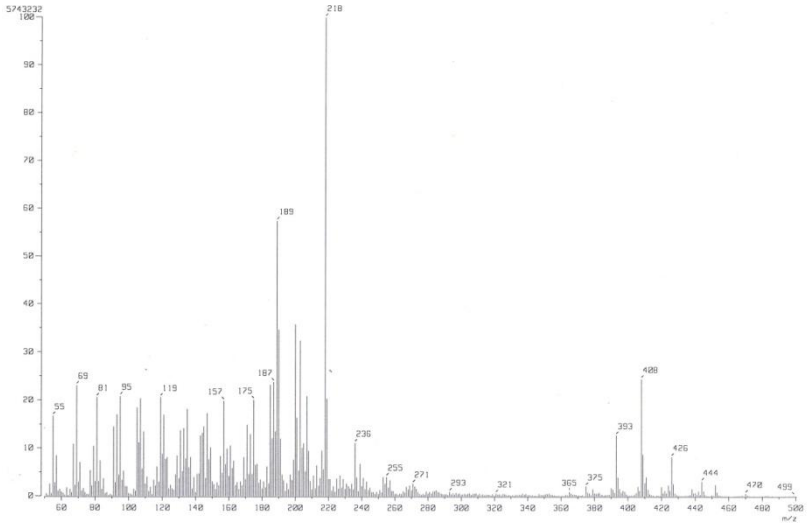

Fig. 19. EIMS spectrum of compound **2**

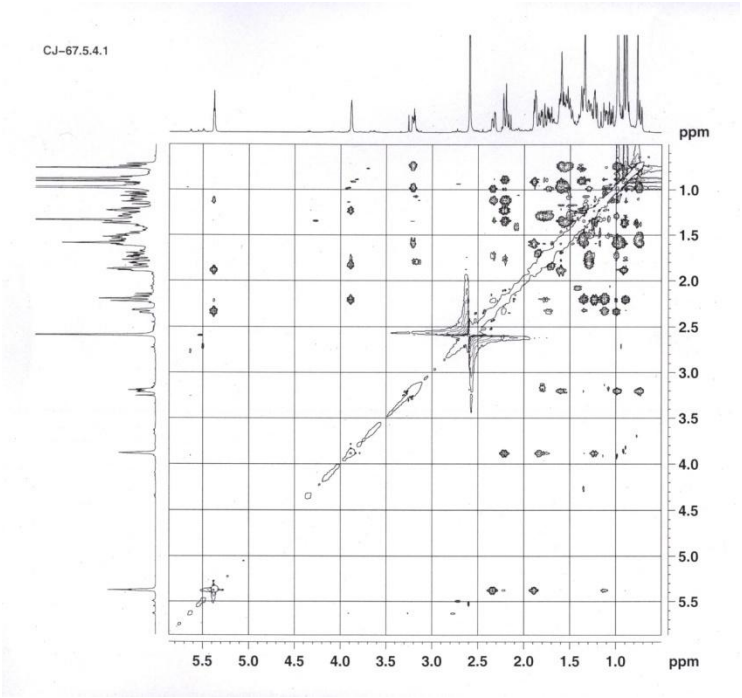

Fig. 20. ^{1}H-^{1}H- NOESY spectrum of compound **2**

Table 2. ^{1}H (500 MHz) and ^{13}C (125 MHz) -NMR data of compound **2**[a] in $CDCl_3$

Position	δ_H mult. (*J* in Hz)	δ_C	HMBC (H→C)
1	1.64 m 1.55 m	38.46	C-2, C-3, C-10
2	1.64 m 1.55 m	27.17	C-1, C-3, C-10
3	3.23 dd (11.3, 3.9)	78.95	C-1, C-2, C-4, C-5, C-24
4		38.75	
5	0.78 brs	55.20	C-3, C-6, C-23, C-24, C-25
6	1.59 m 1.39 m	18.29	C-5, C-7, C-23
7	1.53 m 1.40 s	32.96	C-6, C-8, C-14, C-26
8		39.53	
9	1.62 dd (10.5, 7.0)	46.72	C-8, C-10, C-11, C-25, C-26
10		37.01	
11	1.89 m	23.50	C-9, C-12
12	5.40 brs	124.68	C-11, C-18
13		142.31	
14		41.22	
15	2.22 d (13.2) 1.25 d (12.5)	34.49	C-14, C-16, C-17, C-27
16	3.91 brs	77.97	C-14, C-15, C-17, C-18, C-22
17		71.63	
18	2.36 dd (14.1, 3.2)	47.94	C-12, C-13, C-16, C-17, C-19
19	2.19 m 1.14 m	47.53	C-18, C-20, C-29, C-30
20		30.75	
21	1.80 m 1.34 m	37.02	C-22, C-29, C-30
22	1.85 m 1.73 m	36.10	C-21, C-16, C-17
23	1.00 s	28.11	C-3, C-4, C-5, C-24
24	0.79 s	15.62	C-4, C-5, C-23
25	0.93 s	15.43	C-1, C-5, C-9, C-10
26	0.91 s	17.23	C-7, C-8, C-9, C-14
27	1.37 s	26.84	C-8, C-13, C-14, C-15
28			
29	0.91 s	32.47	C-19, C-20, C-21, C-30
30	1.01 s	24.48	C-19, C-20, C-21, C-29

[a] Assignments were based on HMBC, HSQC, NOESY experiments

3.1.3. Structural determination of compound 3

Compound **3** was obtained as a brown amorphous powder with positive optical rotation ($[\alpha]_D^{25}$ +26.8 in $CHCl_3$). The positive ion HRFABMS spectrum revealed a quasimolecular ion peak at *m/z* 541.3517 $[M + Na]^+$ (calcd 541.3505), consistent with a molecular formula of $C_{31}H_{50}O_6$. In addition, IR absorption bands indicated the existence of hydroxy (3374 cm^{-1}), ester (1740 cm^{-1}), carbonyl (1710 cm^{-1}), and olefinic (1623 cm^{-1}) functional groups. The ^1H NMR (Table 3) showed six methyl singlets (δ_H 0.89, 1.14, 1.16, 1.20, 1.24, 1.29), one carboxymethyl singlet (δ_H 3.57), two oxymethylene signals (δ_H 4.01, 3.47; 3.14) and one olefinic methine signal (δ_H 5.50). The ^{13}C NMR spectrum (Table 3) exhibited 31 carbon signals including one carboxymethyl (δ_C 51.54), one ketone group (δ_C 213.59), two olefinic carbons (δ_C 125.03, 142.37), two oxymethylenes (δ_C 70.85, 74.13), one oxygenated quaternary carbon (δ_C 75.38), six methyls, nine methylenes, three methines and five quaternary carbons. The above findings suggest that compound **3** is a tetracyclic triterpene with the occurrence of 3,4-*seco*-oleanane type skeleton.[87] It was further confirmed by HMBC correlations from δ_H 2.48 and 1.66 (H_2-1), 2.61 and 2.19 (H_2-2), and 3.57 (OMe) to δ_C 175.30 (C-3); from δ_H 1.29 (H_3-23) and 1.24 (H_3-24) to δ_C 75.38 (C-4) and 52.38 (C-5); and from δ_H 1.16 (H_3-25) to δ_C 35.46 (C-1), 52.38 (C-5), 38.93 (C-9) and 41.82 (C-10). These correlations also confirmed the attachments of a carboxymethyl and a hydroxy group at C-3 and C-4 positions, respectively. The presence of a ketone group at C-16 position was determined by the HMBC correlation from H_2-15 (δ_H 2.76, 1.73), H-22 (δ_H 1.23) and H_2-28 (δ_H 4.01, 3.47) to ketocarbonyl carbon at δ_C 213.59. Next, HMBC correlation from an oxymethylene proton signal at δ_H 3.14 to methyl carbon (δ_C 19.48), to C-19 (δ_C 43.37), to C-20 (δ_C 36.74) and to C-21 (δ_C 30.74) indicated that this oxymethylene group was located at C-29 or C-30 position. However, the up field chemical shift of the methyl carbon at δ_C 19.48 suggested that it was C-

30, and, therefore the oxymethylene group was placed at C-29. These assignments were confirmed by NOESY correlations of H-18β (δ_H 2.60) with H_3-30 (δ_H 0.89) and H-12 (δ_H 5.50) (Fig. 21). Moreover, typical signals of another oxymethylene group at C-28 position were observed at δ_H 4.01 and 3.47, and δ_C 70.85, respectively. It was further supported by HMBC correlations from H_2-28 (δ_H 4.01, 3.47) to C-16 (δ_C 213.59), C-17 (δ_C 54.59), C-18 (δ_C 46.75) and C-22 (δ_C 25.84). Thus, compound **3** was determined as 4,28,29-trihydroxy-16-oxo-3,4-*seco*-olean-12-ene-3-oic acid methyl ester and named camelliaolean A.

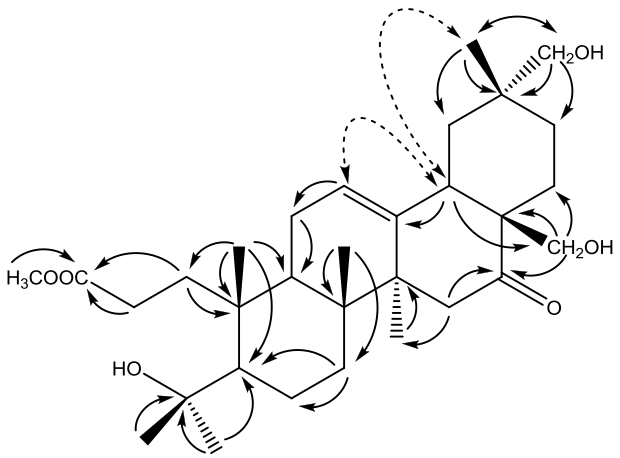

Fig. 21. Key HMBC (H→C) and NOESY (H⋯➤H) correlations of compound **3**

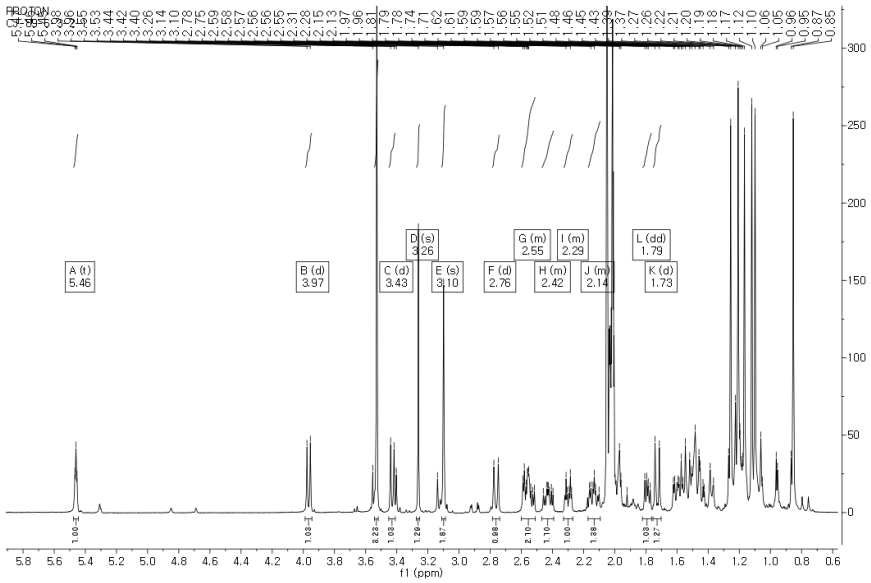

Fig. 22. ^{1}H-NMR (acetone-d_6 500 MHz) spectrum of compound **3**

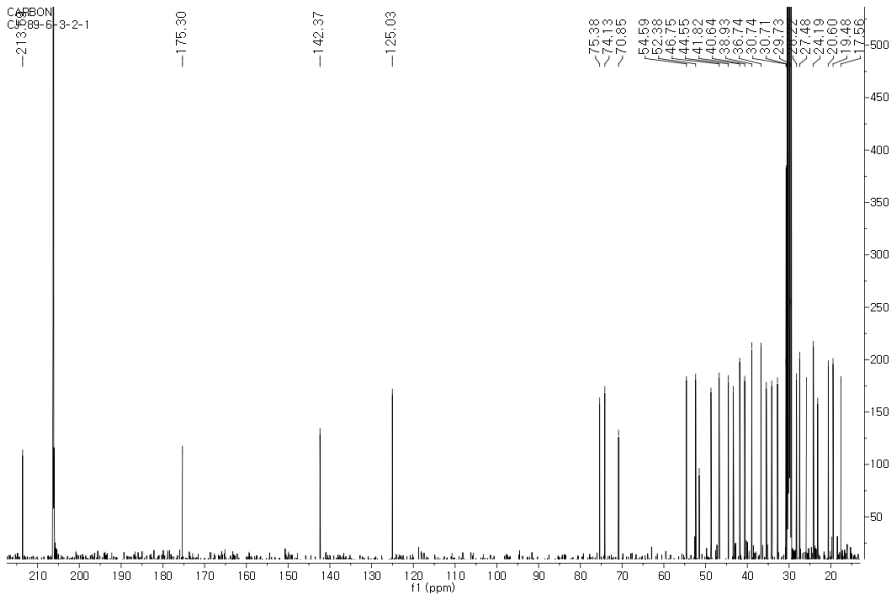

Fig. 23. ^{13}C-NMR (acetone-d_6 125 MHz) spectrum of compound **3**

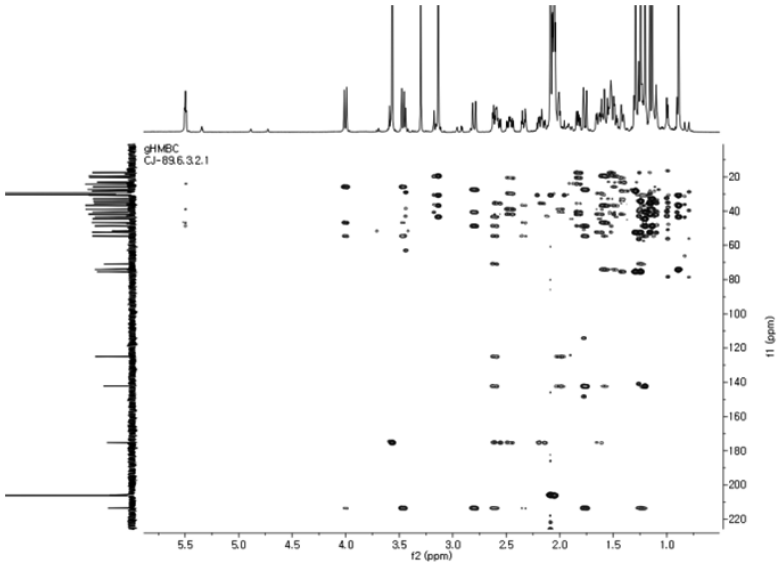

Fig. 24. HMBC spectrum of compound **3**

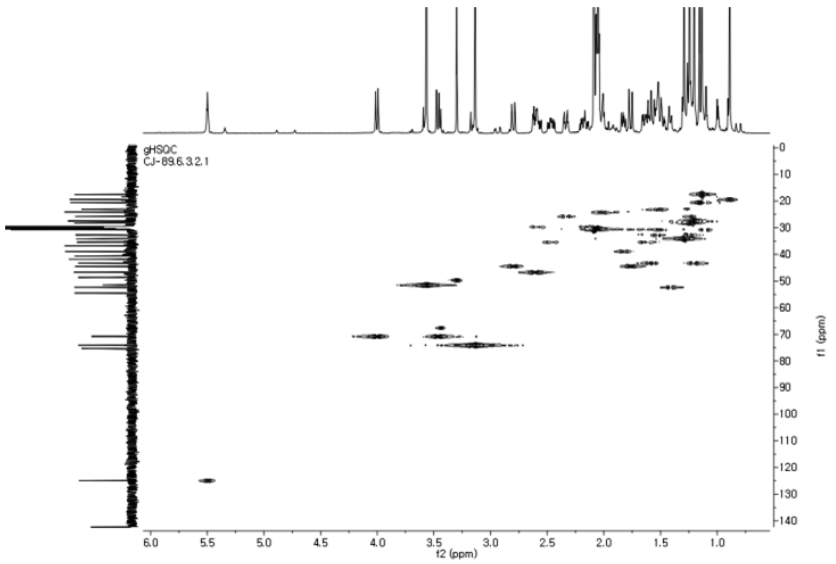

Fig. 25. HSQC spectrum of compound **3**

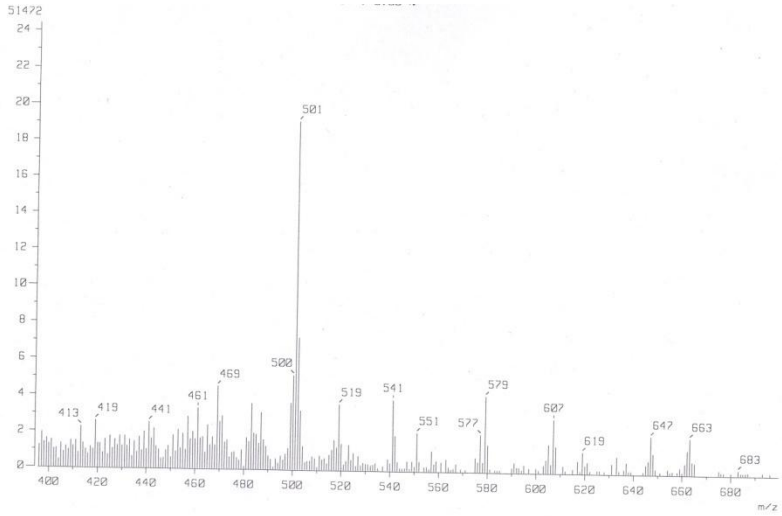

Fig. 26. FABMS spectrum of compound **3**

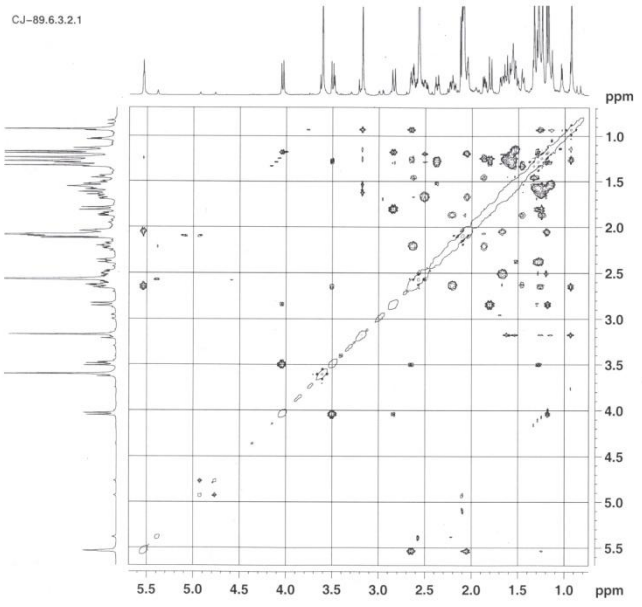

Fig. 27. ^{1}H-^{1}H- NOESY spectrum of compound **3**

Table 3. ^{1}H (500 MHz) and ^{13}C (125 MHz) -NMR data of compound **3**[a] in acetone-d_6

Position	δ_H mult. (*J* in Hz)	δ_C	HMBC (H→C)
1	2.48 m	35.46	C-2, C-3, C-10
	1.66 m		
2	2.61 m	29.73	C-1, C-3, C-10
	2.19 m		
3		175.30	
4		75.38	
5	1.42 brs	52.38	C-6, C-23, C-24, C-25
6	1.60 m	23.15	C-5, C-7, C-23
	1.55 m		
7	1.51 m	32.78	C-6, C-8, C-14, C-26
	1.27 m		
8		40.64	
9	1.79 dd (10.9, 6.6)	38.93	C-8, C-10, C-11, C-25, C-26
10		41.82	
11	2.02 m	24.19	C-9, C-12
12	5.50 t (3.5)	125.03	C-11, C-18
13		142.37	
14		48.71	
15	2.76 d (14.1)	44.55	C-14, C-16, C-17, C-27
	1.73 d (14.0)		
16		213.59	
17		54.59	
18	2.60 dd (14.1, 3.4)	46.75	C-12, C-13, C-16, C-17, C-19, C-28
19	1.59 m	43.37	C-18, C-20, C-29, C-30
	1.23 m		
20		36.74	
21	1.50 m	30.74	C-22, C-29, C-30
	1.50 m		
22	2.33 m	25.84	C-21, C-16, C-17
	1.23 m		
23	1.29 s	34.16	C-4, C-5, C-24
24	1.24 s	28.22	C-4, C-5, C-23
25	1.16 s	20.60	C-1, C-5, C-9, C-10
26	1.14 s	17.56	C-7, C-8, C-9, C-14
27	1.20 s	27.48	C-8, C-13, C-14, C-15
28	4.01 d (10.9)	70.85	C-16, C-17, C-18, C-22
	3.47 d (10.9)		
29	3.14 brs	74.13	C-19, C-20, C-21, C-30
30	0.89 s	19.48	C-19, C-20, C-21, C-29
COO<u>CH</u>$_3$	3.57 s	51.54	C-3

[a] Assignments were based on HMBC, HSQC, NOESY experiments

3.1.4. Structural determination of compound 4

Compound **4,** a white, amorphous powder, showed positive optical rotation ($[\alpha]_D^{25}$ +35.1 in $CHCl_3$). Its IR spectrum displayed intense absorption bands for hydroxy (3363 cm^{-1}), ester (1742 cm^{-1}), and carbonyl (1713 cm^{-1}) functionalities. In addition, the molecular formula of **4** was determined as $C_{30}H_{48}O_6$, on the basis of HRFABMS spectrum, which showed a quasimolecular ion peak at *m/z* 527.3350 $[M + Na]^+$ (calcd for $C_{30}H_{48}O_6Na^+$: 527.3349), 14 mass unit less than that of **3**. The detailed analysis of ^1H and ^{13}C NMR spectral data (Table 4) as well as HMBC and HSQC correlation (Fig. 28) revealed that compound **4** was also a 3,4-*seco*-oleanane type triterpene, closely similar to **3**. However, compound **4** differed from **3** at C-7, C-17, and C-29 positions. The ^1H and ^{13}C NMR spectrum of **4** showed the presence of oxymethine proton signal at δ_H 3.78 (1 H, dd, J= 11.4, 4.1 Hz) with corresponding carbon signal at δ_C 72.34 at C-7 position which was supported by HMBC correlations from δ_H 3.78 to C-6 (δ_C 33.42), C-8 (δ_C 44.73), C-14 (δ_C 48.91) and C-26 (δ_C 10.37). The NOE correlation between proton pair H-7α and H-5, H-6α, H_3-27 as well as the high coupling constant (J= 11.4, 4.1 Hz) confirmed this hydroxy group as β-oriented (Fig. 28). A hydroxy group attachment at C-17 position of compound **4** was also concluded from the HMBC correlations from H-15β (δ_H 2.21) to C-17 (δ_C 76.28); from H-18 (δ_H 2.76) to C-17 (δ_C 76.28); and from H_2-22 (δ_H 2.10, 1.46) to C-17 (δ_C 76.28). Finally, the oxymehylene group at C-29 position in **3** was substituted by a methyl group (δ_H 0.88, δ_C 32.38) in compound **4.** These conclusions were also confirmed by the HMBC correlations from H_3-29 (δ_H 0.88) to C-19 (δ_C 47.02), C-20 (δ_C 30.79), C-21 (δ_C 36.38), and C-30 (δ_C 23.53). Therefore, the chemical structure of compound **4** was designated as 4,7β,17-trihydroxy-16-oxo-3,4-*seco*-olean-12-ene-3-oic acid methyl ester and named camelliaolean B.

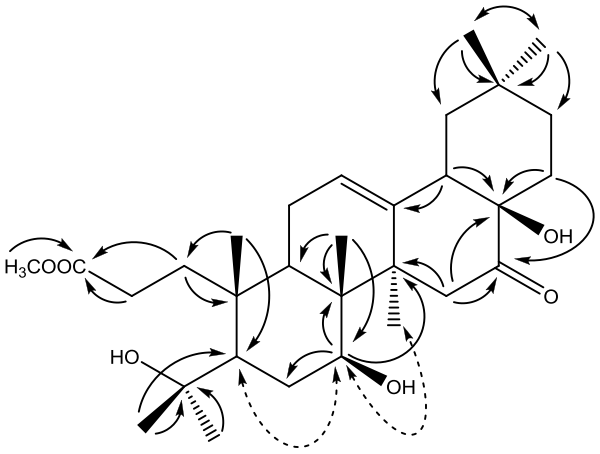

Fig. 28. Key HMBC (H→C) and NOESY (H⋯➝H) correlations of compound **4**

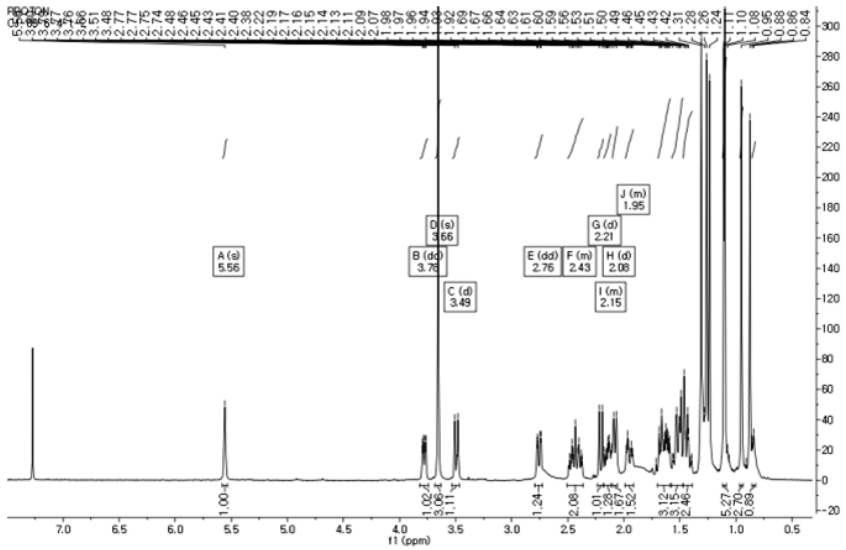

Fig. 29. ^{1}H-NMR ($CDCl_3$ 500 MHz) spectrum of compound **4**

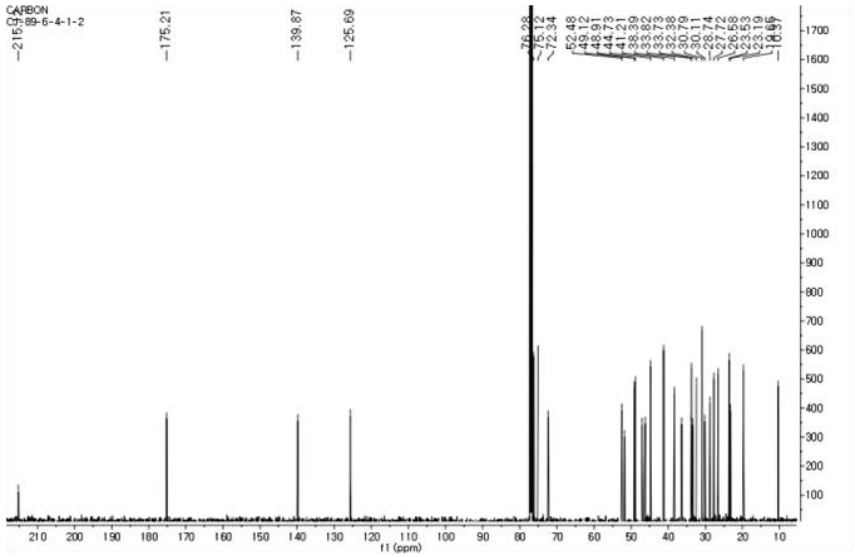

Fig. 30. ^{13}C-NMR ($CDCl_3$ 125 MHz) spectrum of compound **4**

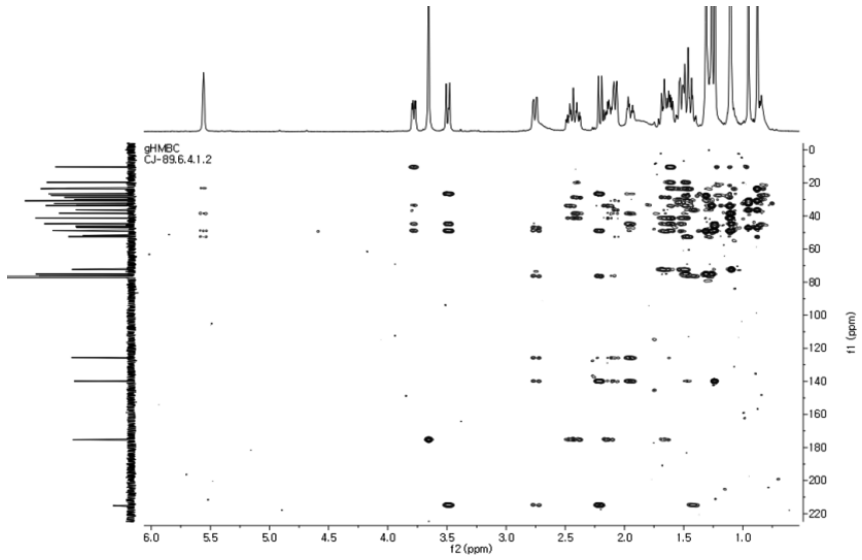

Fig. 31. HMBC spectrum of compound **4**

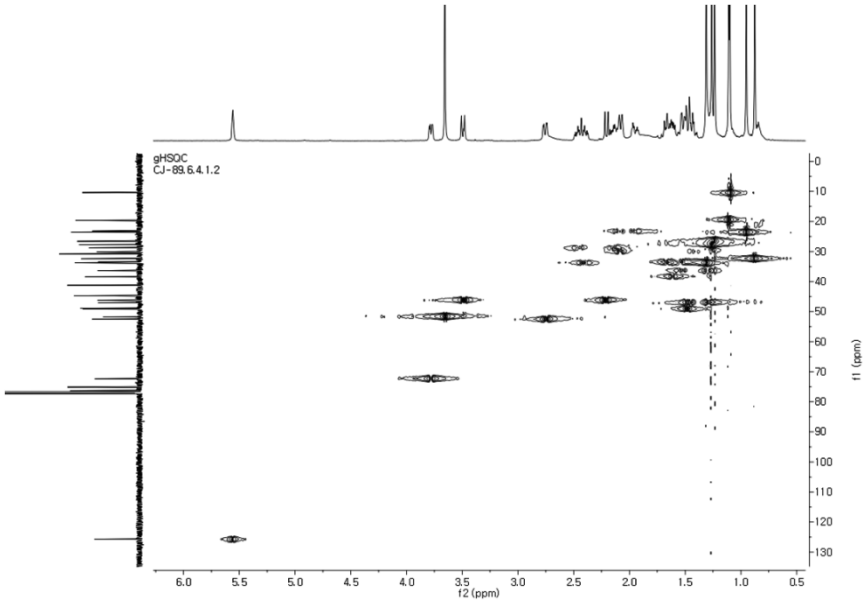

Fig. 32. HSQC spectrum of compound **4**

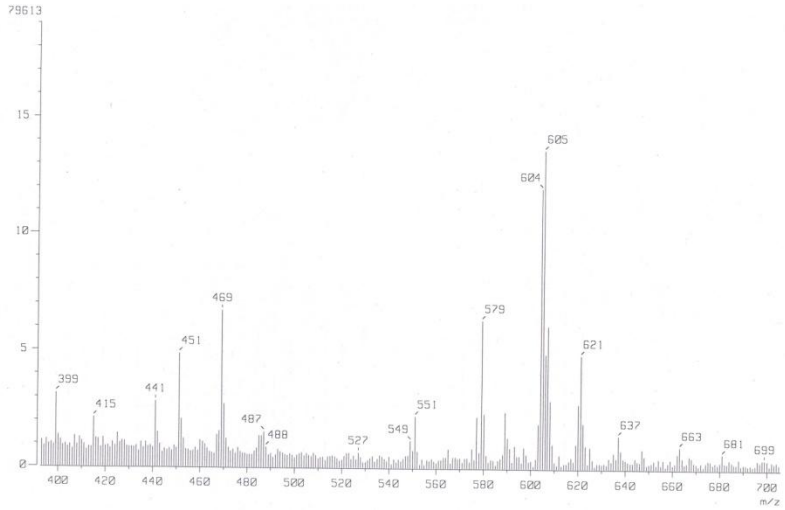

Fig. 33. FABMS spectrum of compound **4**

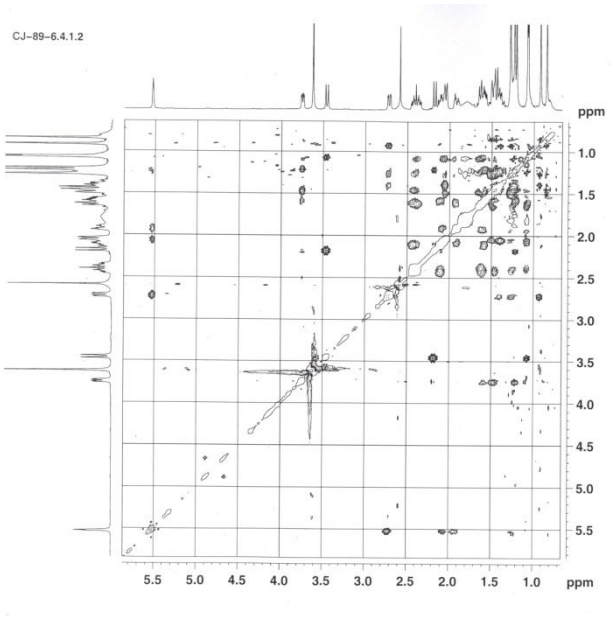

Fig. 34. ^{1}H-^{1}H- NOESY spectrum of compound **4**

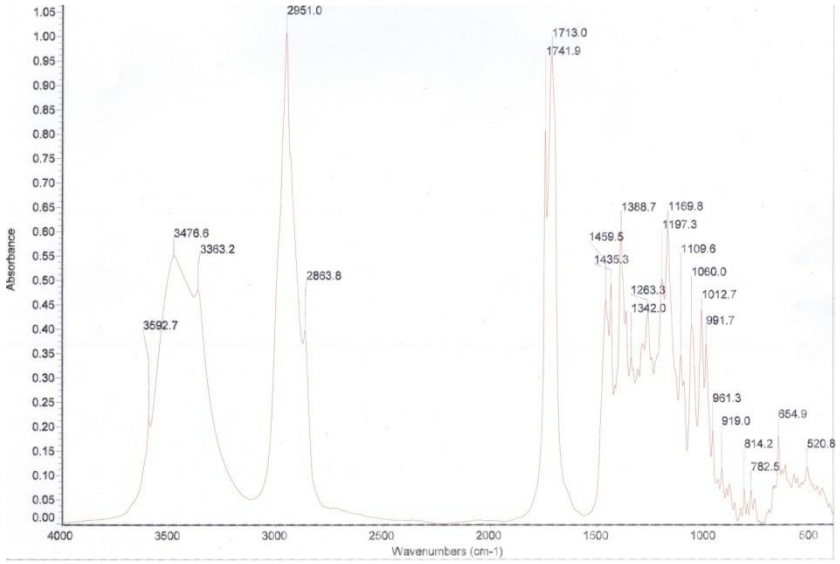

Fig. 35. IR (KBr) spectrum of compound **4**

Table 4. ^{1}H (500 MHz) and ^{13}C (125 MHz) -NMR data of compound **4**[a] in $CDCl_3$

Position	δ_H mult. (*J* in Hz)	δ_C	HMBC (H→C)
1	2.43 m	33.82	C-2, C-3, C-10
	1.66 m		
2	2.43 m	28.74	C-1, C-3, C-10
	2.14 m		
3		175.21	
4		75.12	
5	1.50 m	49.12	C-6, C-23, C-24, C-25
6	1.65 m	33.42	C-5, C-7, C-23
	1.50 m		
7	3.78 dd (11.4, 4.1)	72.34	C-6, C-8, C-14, C-26
8		44.73	
9	1.64 dd (11.1, 5.2)	38.39	C-8, C-10, C-11, C-25, C-26
10		41.21	
11	2.11 m	23.19	C-9, C-12
	1.95 m		
12	5.56 brs	125.69	C-11, C-18
13		139.87	
14		48.91	
15	3.49 d (14.3)	46.22	C-14, C-16, C-17, C-27
	2.21 d (14.3)		
16		215.12	
17		76.28	
18	2.76 dd (14.2, 3.5)	52.48	C-12, C-13, C-16, C-17, C-19
19	1.48 m	47.02	C-18, C-20, C-29, C-30
	1.28 m		
20		30.79	
21	1.55 m	36.38	C-22, C-29, C-30
	1.28 m		
22	2.10 m	30.11	C-21, C-16, C-17
	1.46 m		
23	1.31 s	33.73	C-4, C-5, C-24
24	1.26 s	27.72	C-4, C-5, C-23
25	1.11 s	19.65	C-1, C-5, C-9, C-10
26	1.10 s	10.37	C-7, C-8, C-9, C-14
27	1.24 s	26.58	C-8, C-13, C-14, C-15
28			
29	0.88 s	32.38	C-19, C-20, C-21, C-30
30	0.95 s	23.53	C-19, C-20, C-21, C-29
$COO\underline{CH_3}$	3.66 s	51.76	C-3

[a] Assignments were based on HMBC, HSQC, NOESY experiments

3.1.5. Structural determination of compound 5

Compound **5** was obtained as a white amorphous powder with positive optical rotation ($[\alpha]_D^{25}$ +24.7 in $CHCl_3$). The positive ion HRFABMS spectrum revealed a quasimolecular ion peak at *m/z* 525.3188 $[M + Na]^+$ (calcd 525.3192), consistent with a molecular formula of $C_{30}H_{46}O_6$. In addition, IR absorption bands indicated the existence of hydroxy (3370 cm^{-1}), ester (1735 cm^{-1}), carbonyl (1713 cm^{-1}), and olefinic (1628 cm^{-1}) functional groups. The ^1H NMR (Table 5) showed four tertiary methyls (δ_H 0.95, 0.96, 1.17, 1.25), a vinyl methyl (δ_H 1.77), an exomethylene [δ_H 4.90, 4.73 (each s)], an oxymethine (δ_H 3.87), a carboxymethyl (δ_H 3.59), an oxymethylene (δ_H 3.14) and an olefinic methine signal (δ_H 5.48). The ^{13}C NMR (Table 5) spectrum exhibited 30 carbon signals including a carboxymethyl (δ_C 51.75), a ketone group (δ_C 214.78), two olefinic carbons (δ_C 124.99, 142.64), two exomethylene carbons (δ_C 114.62, 147.34), an oxymethylene carbon (δ_C 73.88), an oxygenated methine carbon (δ_C 72.11), an oxygenated quaternary carbon (δ_C 76.88), four tertiary methyls, one vinyl methyl, eight methylenes, three methines and four quaternary carbons. The above findings accounted for four out of the eight degrees of unsaturation, suggesting that compound **5** is a tetracyclic oleanane type triterpene.[87] The occurrence of 3,4-*seco*-oleanane type skeleton was elucidated from the following HMBC correlations: δ_H 1.60 (H_2-1), 2.45 and 2.14 (H_2-2), and 3.59 (OMe) with δ_C 174.44 (C-3); δ_H 4.90 and 4.73 (H_2-23) and 1.77 (H_3-24) with δ_C 48.46 (C-5); δ_H 0.96 (H_3-25) with δ_C 34.71 (C-1), 48.46 (C-5), 38.28 (C-9), and 40.22 (C-10). These correlations also confirmed the attachment of a carboxymethyl group at C-3 position. Further detailed HMBC, HSQC and ^1H-^1H NOESY confirmed that compound **5** is a 3,4-*seco*-oleanane type triterpenoid. The HMBC correlations of H_2-15 (δ_H 3.56, 2.23), and H-22 (δ_H 1.44) with ketocarbonyl carbon at δ_C 214.78 confirmed the presence of a ketone group at C-16 position. Next, likewise compound **4** one oxymethine signal was also observed for compound **5** at C-7

position, with proton signal at δ_H 3.87 (1 H, dd, J= 11.2, 4.3 Hz) and corresponding carbon signal at δ_C 72.11. It was further evidenced by HMBC correlations from δ_H 3.87 to C-6 (δ_C 35.83), C-8 (δ_C 45.59), C-14 (δ_C 50.12) and C-26 (δ_C 10.99) (Fig. 36). The relative configuration of this hydroxy group was confirmed as β-orientation by comparison of chemical shifts of carbon and proton signals with that of compound **4**. Next, HMBC correlation from an oxymethylene proton signal at δ_H 3.15 to methyl carbon (δ_C 19.45), to C-19 (δ_C 43.21), to C-20 (δ_C 36.68) and to C-21 (δ_C 32.21) indicated that this oxymethylene group was located at C-29 or C-30 position. However, likewise compound **3**, the upfield chemical shift of the methyl carbon at δ_C 19.45 suggested that it was C-30, and, therefore the oxymethylene group was placed at C-29. Similar chemical shifts of carbon and proton signals and HMBC correlation with that of compound **3** also confirmed these assignments. Furthermore, the HMBC correlation between H-15β (δ_H 2.23), H-18 (δ_H 2.80), H_2-22 (δ_H 1.44, 2.07) and oxygenated carbon (δ_C 76.88) inferred the attachment of another hydroxy group at C-17 position. Based on the above findings, the chemical structure of compound **5** was determined as 7β,17,29-trihydroxy-16-oxo-3,4-*seco*-olean-4(23),12(13)-diene-3-oic acid methyl ester and named camelliaolean C.

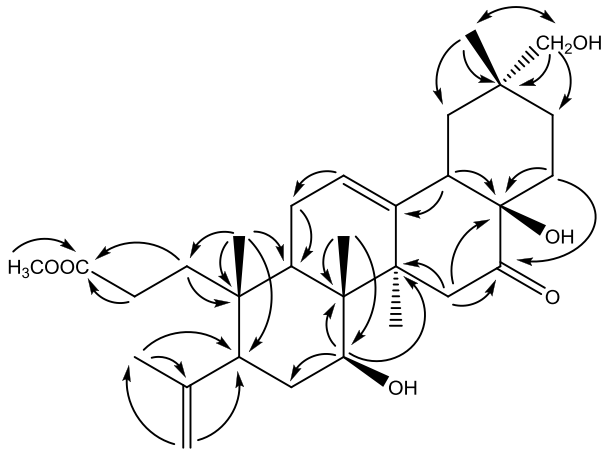

Fig. 36. Key HMBC (H→C) correlation of compound **5**

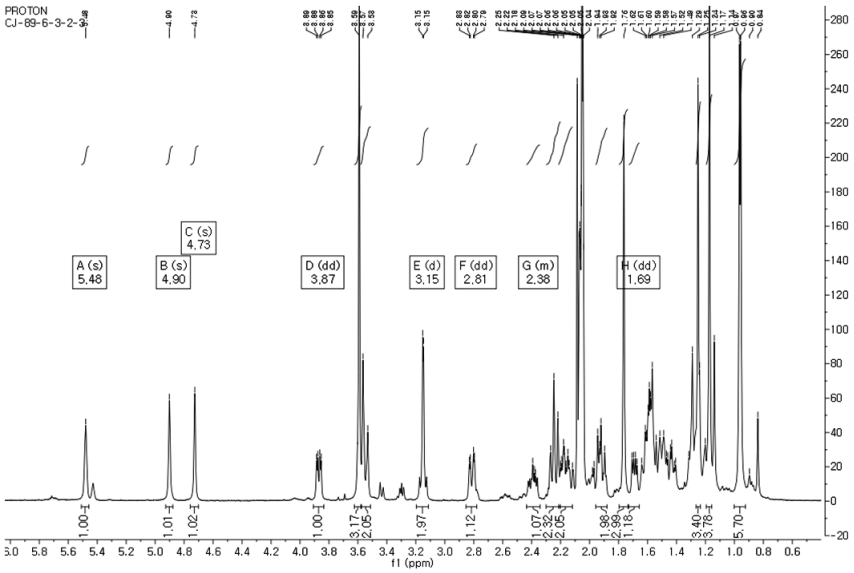

Fig. 37. ^{1}H-NMR (acetone-d_6 500 MHz) spectrum of compound **5**

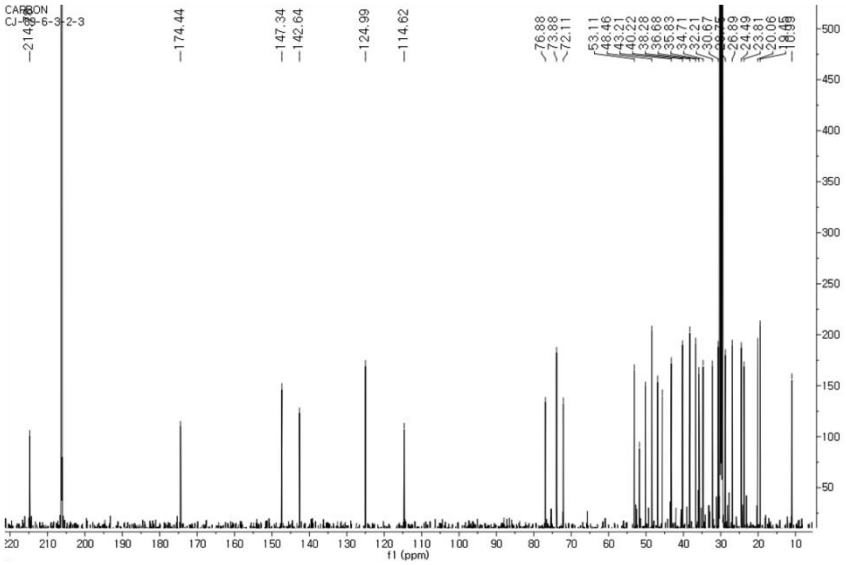

Fig. 38. ^{13}C-NMR (acetone-d_6 125 MHz) spectrum of compound **5**

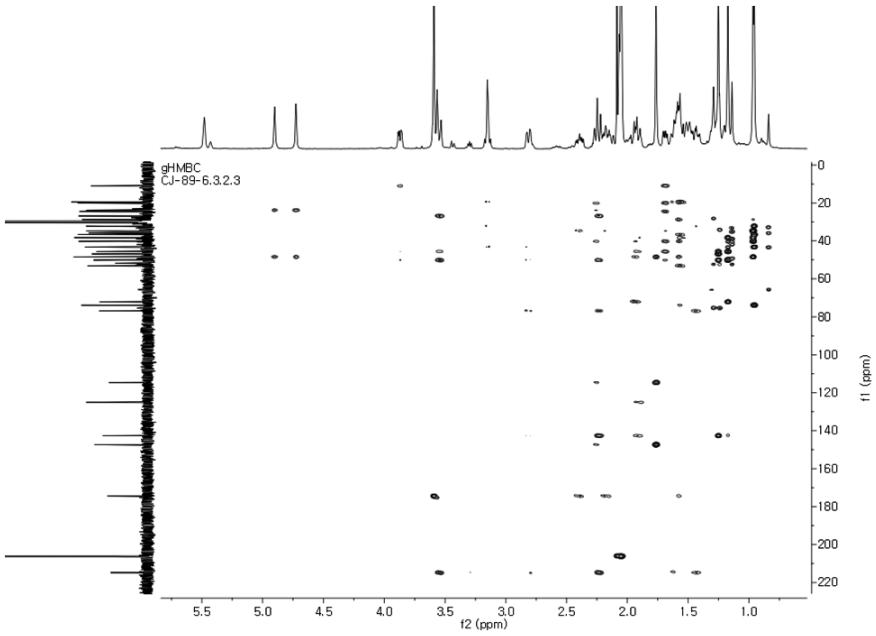

Fig. 39. HMBC spectrum of compound **5**

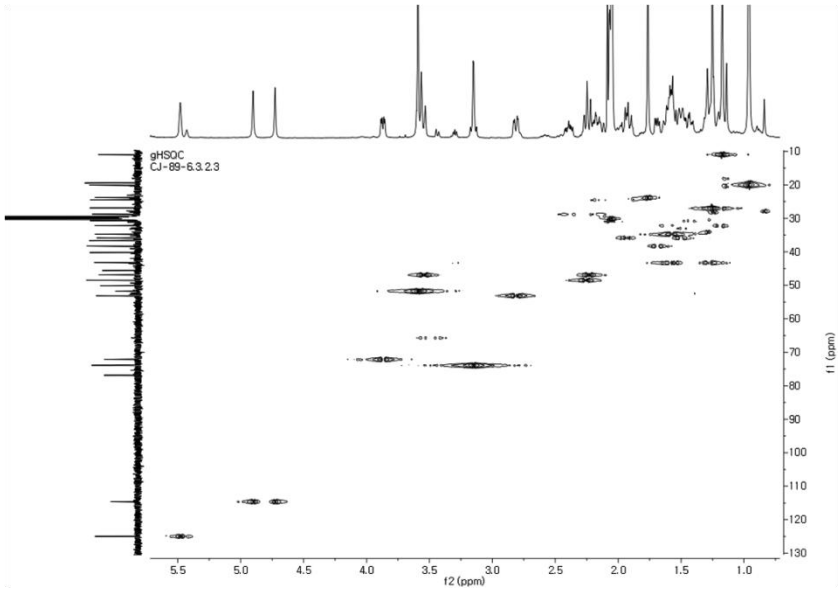

Fig. 40. HSQC spectrum of compound **5**

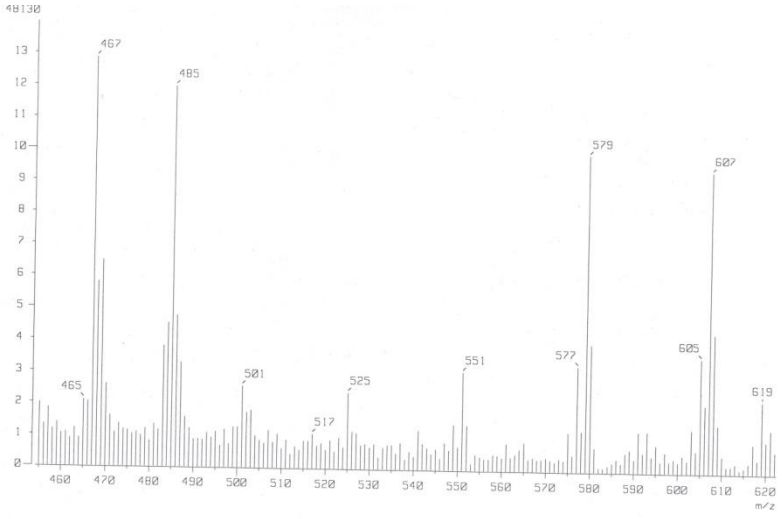

Fig. 41. FABMS spectrum of compound **5**

Table 5. ^{1}H (500 MHz) and ^{13}C (125 MHz) -NMR data of compound **5**[a] in acetone-d_6

Position	δ_H mult. (*J* in Hz)	δ_C	HMBC (H→C)
1	1.60 m	34.71	C-2, C-3, C-10
	1.60 m		
2	2.45 m	28.75	C-1, C-3, C-10
	2.14 m		
3		174.44	
4		147.34	
5	2.26 m	48.46	C-6, C-23, C-24, C-25
6	1.95 m	35.83	C-5, C-7
	1.52 m		
7	3.87 dd (11.2, 4.3)	72.11	C-6, C-8, C-14, C-26
8		45.59	
9	1.69 dd (11.7, 5.6)	38.28	C-8, C-10, C-11, C-25, C-26
10		40.22	
11	2.19 m	24.49	C-9, C-12
	2.19 m		
12	5.48 brs	124.99	C-9, C-11, C-14, C-18
13		142.64	
14		50.12	
15	3.56 d (14.2)	46.87	C-14, C-16, C-17, C-27
	2.23 d (14.2)		
16		214.78	
17		76.88	
18	2.80 dd (14.2, 3.8)	53.11	C-12, C-13, C-16, C-17, C-19
19	1.55 m	43.21	C-18, C-20, C-29, C-30
	1.30 m		
20		36.68	
21	1.64 m	32.21	C-22, C-29, C-30
	1.21 m		
22	2.07 m	30.67	C-21, C-16, C-17
	1.44 m		
23	4.90 brs	114.62	C-4, C-5, C-24
	4.73 brs		
24	1.77 s	23.81	C-4, C-5, C-23
25	0.96 s	20.06	C-1, C-5, C-9, C-10
26	1.17 s	10.99	C-7, C-8, C-9, C-14
27	1.25 s	26.89	C-8, C-13, C-14, C-15
28			
29	3.15 d (2.8)	73.88	C-19, C-20, C-21, C-30
30	0.95 s	19.45	C-19, C-20, C-21, C-29
COO$\underline{CH_3}$	3.59 s	51.75	C-3

[a] Assignments were based on HMBC, HSQC experiments

3.1.6. Structural determination of compound 6

Compound **6** was isolated as a brown amorphous powder with positive optical rotation ($[\alpha]_D^{25}$ +28.3 in $CHCl_3$). The positive ion HRFABMS spectrum revealed a quasimolecular ion peak at *m/z* 473.3283 $[M + H]^+$ (calcd 473.3267), consistent with a molecular formula of $C_{29}H_{44}O_5$. In addition, IR spectrum displayed intense absorption bands for hydroxy (3360 cm^{-1}), ester (1730 cm^{-1}), carbonyl (1710 cm^{-1}), and olefinic (1615 cm^{-1}) functionalities. The carbon and proton signals in the ^1H and ^{13}C NMR spectra (Table 6) were superimposable on those of **5** (Table 5)**,** except for the signals around C-3, and C-7 positions. In compound **5,** a carboxymethyl group (δ_C 174.44, 51.75) was appeared at C-3 position, which was substituted by a free carboxy group at δ_C 174.97 in case of **6**. This assignment was further evidenced by HMBC correlations, from H_2-1 (δ_H 1.59, 1.56) and H_2-2 (δ_H 2.40, 2.21) to C-3 (δ_C174.97) (Fig. 42). Finally, at C-7 position, a methylene group was observed for **6** at δ_C 32.50 with corresponding proton signals (δ_H 1.53, 1.28) instead of an oxymethine group for **5**. The HMBC correlation between H-5 (δ_H 2.12), H_3-26 (δ_H 1.18) and C-7 (δ_C 32.50) as well as correlation between H_2-7 (δ_H 1.53, 1.28) and C-6 (δ_C 25.36), C-8 (δ_C 40.38) further confirmed these assignments. The chemical shift values as well as the HMBC and HSQC correlations of other carbon and proton signals were closely similar to **5**. Therefore, based on the above findings, the chemical structure of compound **6** was deduced as 17,29-dihydroxy-16-oxo-3,4-*seco*-olean-4(23),12(13)-diene-3-oic acid and named camelliaolean D.

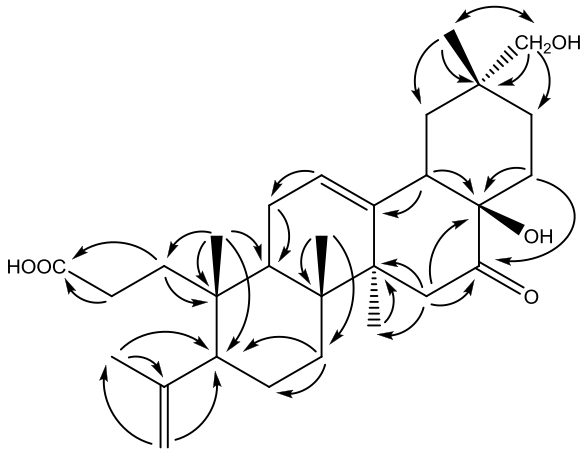

Fig. 42. Key HMBC (H→C) correlation of compound **6**

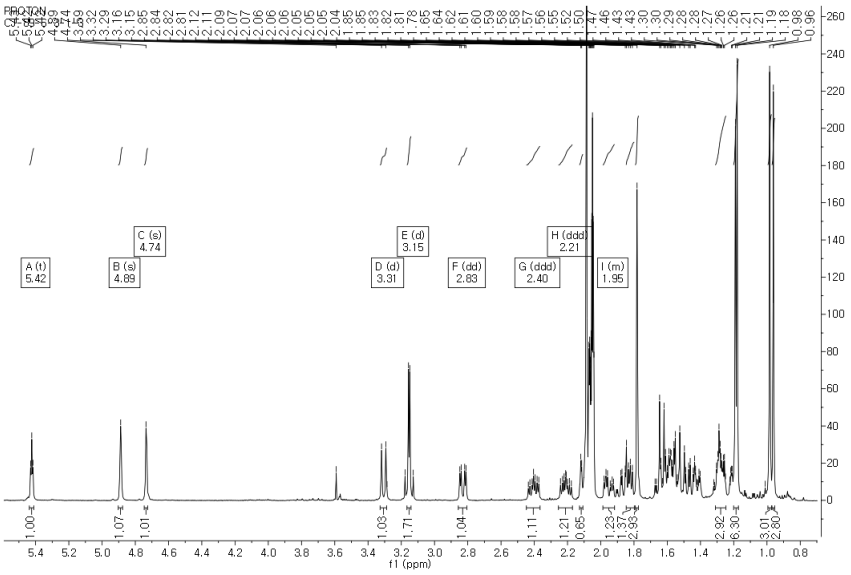

Fig. 43. ^{1}H-NMR (acetone-d_6 600 MHz) spectrum of compound **6**

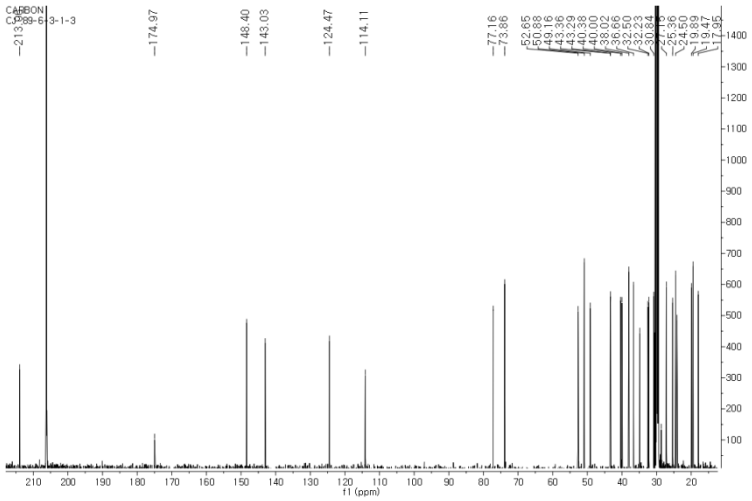

Fig. 44. ^{13}C-NMR (acetone-d_6 150 MHz) spectrum of compound **6**

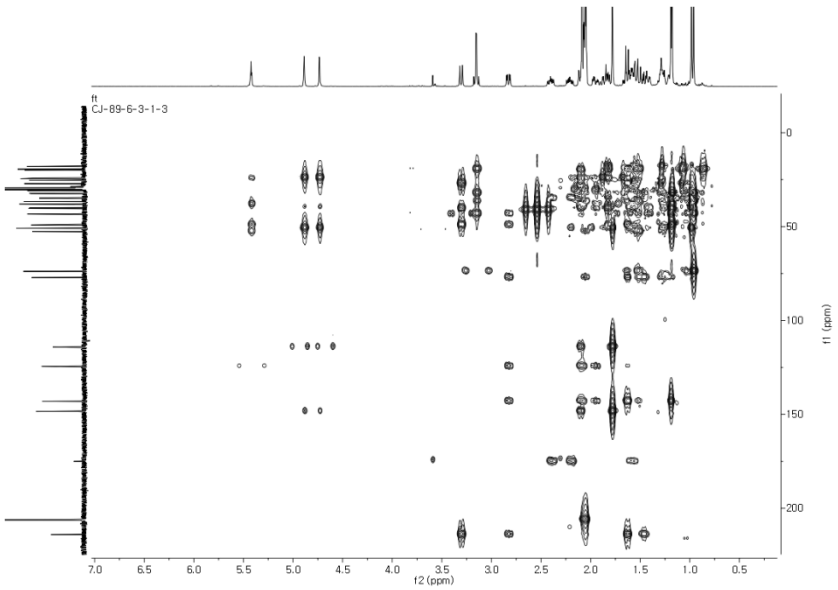

Fig. 45. HMBC spectrum of compound **6**

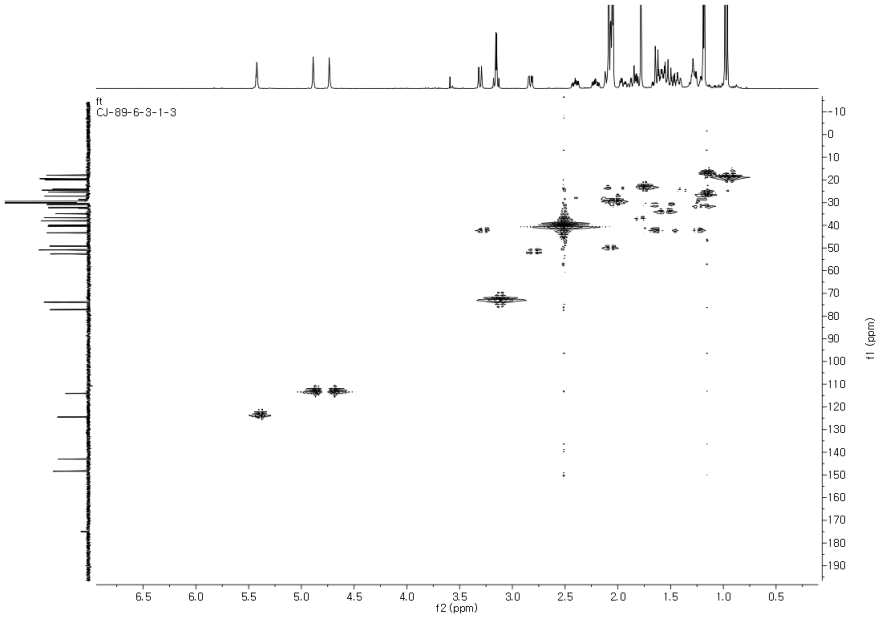

Fig. 46. HSQC spectrum of compound **6**

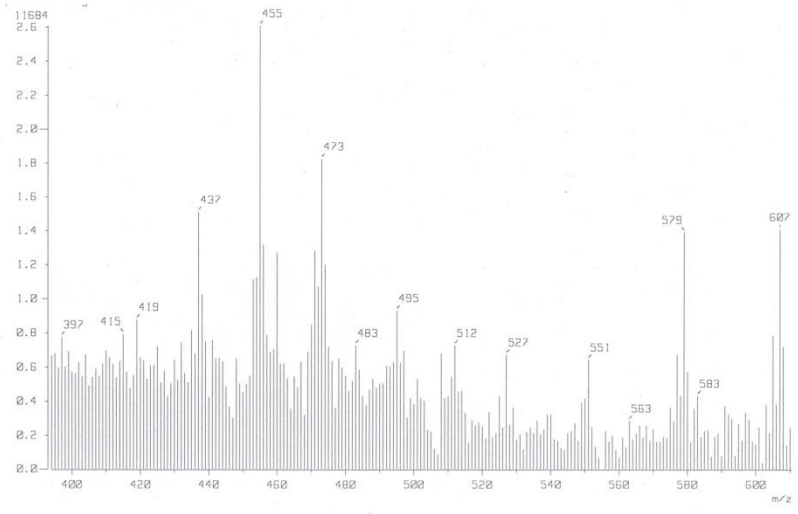

Fig. 47. FABMS spectrum of compound **6**

Table 6. ^{1}H (600 MHz) and ^{13}C (150 MHz) -NMR data of compound **6**[a] in acetone-d_6

Position	δ_H mult. (*J* in Hz)	δ_C	HMBC (H→C)
1	1.59 m 1.56 m	34.87	C-2, C-3, C-10
2	2.40 ddd (15.9, 11.3, 5.0) 2.21 ddd (15.4, 11.3, 6.2)	28.67	C-1, C-3, C-10
3		174.97	
4		148.40	
5	2.12 m	50.88	C-6, C-23, C-24, C-25
6	1.59 m 1.42 m	25.36	C-5, C-7
7	1.53 m 1.28 m	32.50	C-6, C-8, C-14, C-26
8		40.38	
9	1.82 dd (11.5, 5.3)	38.02	C-8, C-10, C-11, C-25, C-26
10		40.00	
11	2.08 m 1.95 m	24.50	C-9, C-12
12	5.42 t (3.5)	124.47	C-9, C-11, C-14, C-18
13		143.03	
14		49.16	
15	3.31 d (13.1) 1.62 d (13.1)	43.36	C-14, C-16, C-17, C-27
16		213.96	
17		77.16	
18	2.83 dd (14.4, 4.1)	52.65	C-12, C-13, C-16, C-17, C-19
19	1.53 m 1.29 m	43.29	C-18, C-20, C-29, C-30
20		36.66	
21	1.64 m 1.21 m	32.23	C-22, C-29, C-30
22	2.07 m 1.45 m	30.84	C-21, C-16, C-17
23	4.89 brs 4.74 brs	114.11	C-4, C-5, C-24
24	1.78 s	24.09	C-4, C-5, C-23
25	0.98 s	19.89	C-1, C-5, C-9, C-10
26	1.18 s	17.95	C-7, C-8, C-9, C-14
27	1.19 s	27.15	C-8, C-13, C-14, C-15
28			
29	3.15 d (3.9)	73.86	C-19, C-20, C-21, C-30
30	0.96 s	19.47	C-19, C-20, C-21, C-29

[a] Assignments were based on HMBC, HSQC experiments

3.2. PTP1B inhibitory effects of isolated compounds 1-14

All isolated compounds from fruit peels of *C. japonica* were evaluated for their inhibitory effects on PTP1B enzyme and the results were summarized in Table 7. The PTP1B enzyme inhibition assay is based on the enzymatic hydrolysis of *p*-nitro phenyl phosphate (*p*-NPP). Upon dephosphorylation by PTP1B enzyme, *p*-NPP is cleaved into *p*-nitrophenol which is estimated by measuring the absorbance at 405 nm. If test compounds inhibit PTP1B enzyme, production of *p*-nitrophenol will be reduced and, therefore, low absorbance will be observed. However, in this study, all oleanane type compounds showed strong to moderate PTP1B inhibitory activity while 3,4-*seco*-oleanane-type compounds did not inhibit PTP1B enzyme even at higher concentration of 50 μM (Table 7). Among oleananes, compounds **2**, **8**, **10**, **11**, and **13** showed strong inhibitory activity (Fig. 48) with IC_{50} values ranging from 3.77 ± 0.11 to 6.40 ± 0.81 μM and the inhibition was concentration dependent. On the other hand, the IC_{50} value for reference ursolic acid was found 3.74 ± 0.31 μM. Interestingly, comparing with reference ursolic acid, similar type very strong inhibition was found for compounds **2** (IC_{50} 3.94 ± 0.29 μM) and **11** (IC_{50} 3.77 ± 0.11 μM). It is noteworthy to mention that, triterpenes especially oleanane-type triterpenes have long been studied and reported for their strong PTP1B inhibitory potential.[88] The oleanane triterpenes from *C. japonica* also showed significant inhibitions on PTP1B enzyme which are consistent with the evidences. Therefore, camellia oleananes especially compounds **2** and **11** might be used for the treatment of PTP1B related diseases including breast cancer.

Table 7. Inhibitory effects of isolated compounds **1-14** on PTP1B enzyme

Compounds[a]	**Inhibitory effect (IC_{50}, µM)**[b]
1	16.23 ± 2.19
2	3.94 ± 0.29
3	NA[c]
4	NA
5	NA
6	> 30
7	> 30
8	6.40 ± 0.81
9	6.97 ± 1.10
10	4.79 ± 0.15
11	3.77 ± 0.11
12	11.62 ± 1.17
13	4.66 ± 0.71
14	5.34 ± 0.42
Ursolic acid[d]	3.74 ± 0.31

NA: Not active.

[a] The purities of compounds for assay were purified by HPLC over 95%

[b]Values are expressed as mean ± SD of three replicates. Seven concentration points were set for establishment of PTP1B inhibition curve to calculate IC_{50} value.

[c] Compounds showed no activity at concentration of 50 µM.

[d] Positive control.

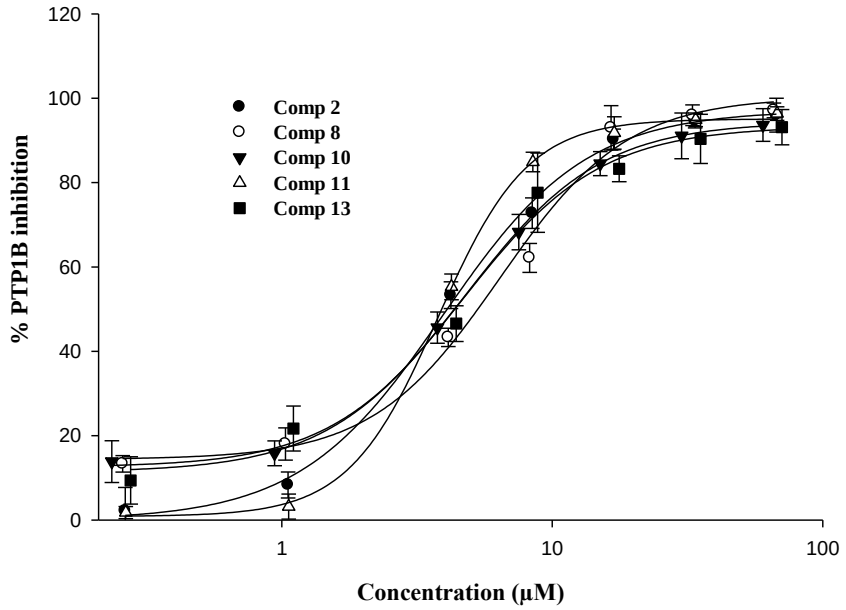

Fig. 48. PTP1B inhibitory effects of the isolated compounds from *C. japonica*. Compounds **2**, **8**, **10, 11,** and **13** showed concentration dependent strong inhibition on PTP1B activity. Ursolic acid was used as positive control which was presented in Table 7. Compound concentrations are displayed on logarithmic scales.

3.3. PTP1B inhibition mode for isolated compounds - Lineweaver-Burk and Dixon plots

Based on the interesting results in PTP1B inhibition assay, two most strong inhibitors (**2**, and **11**) were investigated to determine the mode of inhibition. The double reciprocal Lineweaver-Burk plot and single reciprocal Dixon plot were used for determination of inhibition type of tested compounds. As shown in Fig. 49, both compounds **2,** and **11** showed non-competitive inhibition since increasing the substrate concentrations resulted in a family of lines that did not intersect on the *y*-axis in the Lineweaver-Burk plot (Fig. 49A-B) but intersected at a non-zero point on the negative *x*-axis ($-K_i$) in Dixon plots (Fig. 49C-D). Moreover, from Dixon plots the inhibition constant (K_i) values were determined and found to be 6.59 µM and 3.53 µM for **2** and **8** (Fig. 49C-D), respectively. These K_i values were also in good agreement with IC_{50} values (Table 7). The K_i value is used to characterize and compare the effectiveness of an inhibitor relative to K_m, the binding constant for the substrate. This parameter is especially useful and important in evaluating the potential therapeutic value of inhibitors (drugs) of a given enzyme-catalyzed reaction. The lower the K_i value, the tighter the binding generally is, and hence the more effective an inhibitor is. Therefore, the relatively lower K_i values for compounds **2** and **11** indicated that these compounds might be considered as lead for the development of potential PTP1B inhibitors.

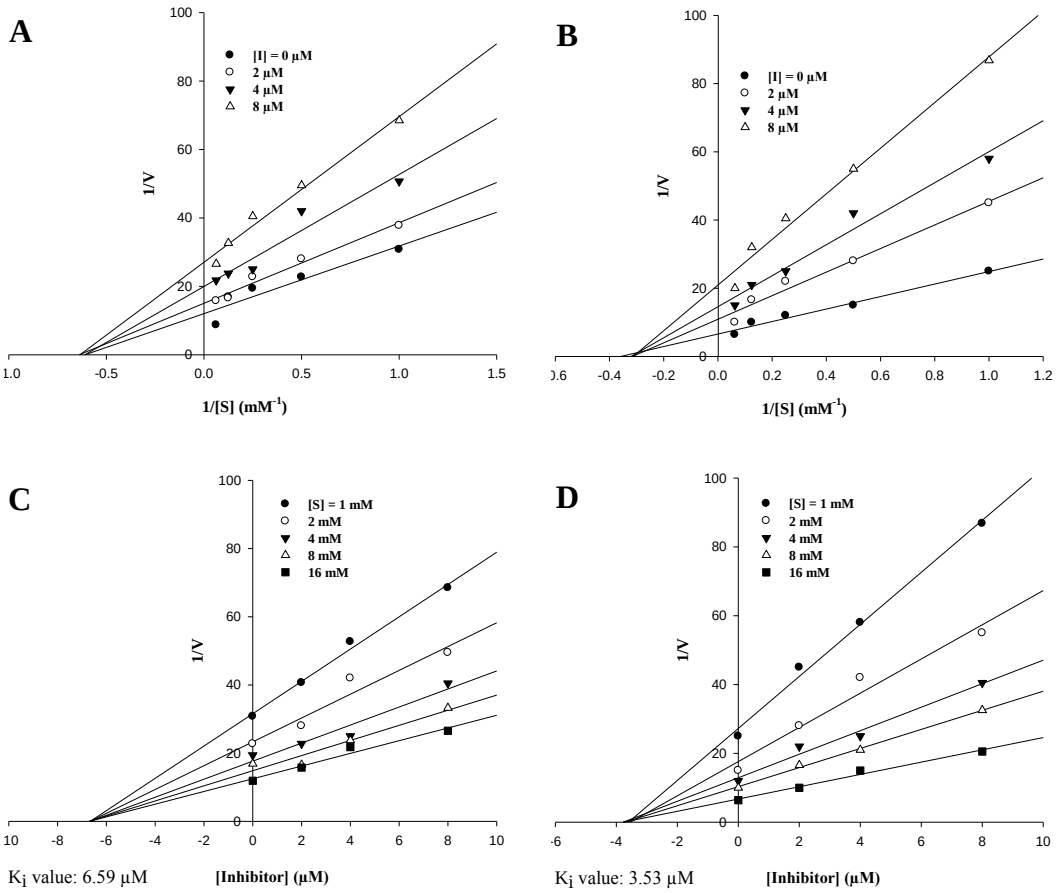

Fig. 49. Graphical determination of inhibition mode for the isolated compounds. (**A**-**B**) Lineweaver-Burk plots for the inhibition of compounds **2** and **11** on the PTP1B-catalyzed hydrolysis of *p*-NPP. The data are expressed as the mean reciprocal of initial velocity for $n = 3$ replicates at each substrate concentration. (**C**-**D**) Dixon plots for compounds **2** and **11** determining the inhibition constant $K_{i.}$ The K_i value was determined from the negative *x*-axis value at the point of the intersection of the five lines. The data are expressed as the mean reciprocal of initial velocity for $n = 3$ replicates at each substrate concentration.

3.4. Growth inhibitory effects of isolated compounds (1-14) against breast cancer cell lines

Breast cancer is the leading cause of cancer death among women worldwide. However, as discussed earlier, recent studies showed that PTP1B inhibitors might play an important role for breast cancer treatment. Hence, based on the interesting results in PTP1B inhibition and kinetics studies, all isolates (**1**-**14**) from *C. japonica* were evaluated for their growth inhibition on three breast cancer cell lines, namely MCF7, MCF7/ADR, and MDA-MB-231. 4-hydroxytamoxifen was used as a positive control. The IC_{50} values of all tested isolates were summarized in Table 8. However, as it is shown in Table 8 and Fig. 50, compounds **2**, **8**, **10**, **11**, and **13** showed very strong cytotoxicity with IC_{50} values ranging from 1.19 ± 0.16 to 8.75 ± 0.72 µM, 0.82 ± 0.23 to 5.17 ± 0.26 µM and 0.51 ± 0.05 to 9.32 ± 0.62 µM against MCF7, MCF7/ADR and MDA-MB-231 cell lines, respectively. These results were also comparable with positive control 4-hydroxytamoxifen (IC_{50} values ranging from 2.39 ± 0.08 to 4.81 ± 0.42 µM). Interestingly, these five compounds also showed very strong PTP1B inhibition, thereby suggesting that these compounds might exhibit cytotoxicity via PTP1B inhibition. Moreover, several previous studies on animal model also showed that PTP1B inhibition was responsible for the amelioration of breast tumorigenesis,[89] which further agreed with these results. On the other hand, the 3,4-*seco*-oleanane type compounds (**3**-**6**) did not show cytotoxicity against any type of cell line. Similar trend was also observed in PTP1B inhibition assay which also support the positive role of PTP1B in breast tumorigenesis. Therefore, the oleanane-type triterpenes from *C. japonica* as PTP1B inhibitors might be used in breast cancer treatment.

Table 8. Growth inhibitory effects of isolated compounds (**1-14**) against breast cancer cell lines

Compounds[a]	**Cell lines/ IC_{50} (µM)**[b]		
	MCF7	**MCF7/ADR**	**MDA-MB-231**
1	> 30	17.37 ± 0.43	16.92 ± 0.65
2	1.96 ± 0.11	1.52 ± 0.16	0.98 ± 0.07
3	NA[c]	NA	NA
4	NA	NA	NA
5	NA	NA	NA
6	NA	NA	NA
7	> 30	> 30	> 30
8	4.95 ± 0.97	2.37 ± 0.46	9.32 ± 0.62
9	11.56 ± 0.35	7.39 ± 0.19	3.32 ± 0.06
10	5.21 ± 0.17	5.17 ± 0.26	4.31 ± 0.18
11	1.19 ± 0.16	0.82 ± 0.23	0.51 ± 0.05
12	15.68 ± 0.54	6.48 ± 0.37	3.44 ± 0.29
13	8.75 ± 0.72	2.51 ± 0.16	2.06 ± 0.34
14	13.55 ±1.44	8.06 ± 0.68	3.15 ± 0.20
4-hydroxytamoxifen[d]	4.81 ± 0.42	2.21 ± 0.20	2.39 ± 0.08

NA: Not active.

[a] The purities of compounds for assay were purified by HPLC over 95%.

[b]Values are expressed as mean ± SD of three replicates.

[c]Compounds showed no activity at concentration of 50 µM.

[d] Positive control.

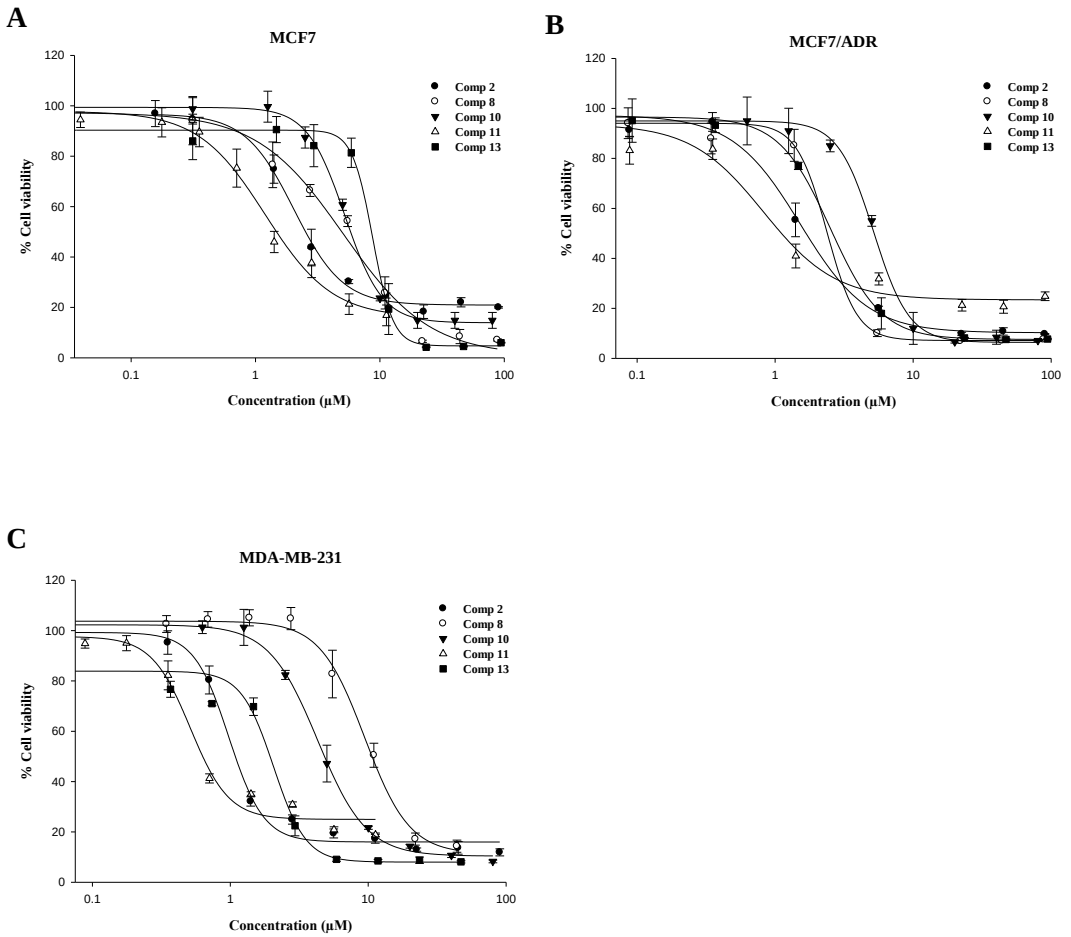

Fig. 50. Growth inhibitory effects of isolated compounds against breast cancer cell lines. Compounds **2, 8, 10, 11,** and **13** showed very strong growth inhibition on (**A**) MCF7 (**B**) MCF7/ADR and (**C**) MDA-MB-231 breast cancer cell lines in a concentration dependent manner. 4-hydroxytamoxifen was used as positive control in all experiments and also presented in Table 8. Concentrations of all compounds are displayed on logarithmic scales. The IC_{50} value was determined from the midpoint (cytotoxic activity = 50%) of the semilog plot.

3.5. Structure activity relationships

Based on the structure activity relationships, it was observed that, the oleanane-type compounds (**1, 2**, and **7**-**14**) (Fig. 6) exhibited both PTP1B inhibitory and cytotoxic activity, while 3,4-*seco*-oleanane type compounds (**3**-**6**) (Fig. 6) showed neither PTP1B inhibition nor cytotoxicity. These results indicated that, A ring in the structure of oleanane type-compounds might have role in inhibitory activity.[90] Of tested oleananes, compounds **2**, **8**, **11**, **13** and **14** with hydroxy group at C-3 or/and carboxy group at C-28 position showed strong PTP1B inhibitory activity and significant cytotoxicity against all cell lines (Tables 7 and 8). Recent studies revealed that 3-OH and 28-COOH are important in determining the pharmacological activities of pentacyclic triterpenes.[91] Moreover, oleanane triterpenes from other plants with -OH at C-3 and -COOH at C-28 positions have also been reported for significant PTP1B inhibition[88, 92] and cytotoxicity against cancer cell lines,[93, 94] which are in good agreement with these results. On the other hand, substitution of C-3 hydroxy group by a ketone group in compounds **1** and **7** reduced the activity considerably in both PTP1B inhibition with IC_{50} values ranging from 16.23 ± 2.19 to >30 μM and cytotoxicity (IC_{50} values ranging from 16.92 ± 0.65 to >30 μM), which was also consistent with the observation in other triterpenoids.[88, 93] Furthermore, similar effect was also observed in compound **12** as the attachments of ketone group at C-12 position also reduced both type activities. However, although acetylation of hydroxy group at C-3 position were reported to reduce activity but in compounds **9** and **10** (Tables 7 and 8) opposite trend was noticed which could be explained by the attachment of -COOH group at C-28 position.[92, 94]

4. Conclusions

Previous studies on other plants showed that pentacyclic triterpenes have potential as PTP1B inhibitors. In addition, they have also been reported to possess cytotoxicity against breast cancer cells. However, there is no report on camellia triterpenes as PTP1B inhibitors with related cytotoxicity against breast cancer cell lines. In this study, bioactivity guided isolation resulted in six new (**1**-**6**) along with eight known (**7**-**14**) oleanane-type triterpenes. Among all, compounds **3**-**6** are of 3,4-*seco*-oleanane type triterpenes and reported for the first time not only from *C. japonica* but also from Camellia genus. In PTP1B enzyme inhibition assay, compounds **2**, **8**, **10**, **11** and **13** showed very strong PTP1B inhibitory potential. Expectedly, these compounds also exhibited strong cytotoxicity against all breast cancer cell lines. Moreover, compounds **2** and **11** were found to possess very strong PTP1B inhibition (non-competitive type) with significant cytotoxicty as compared with positive control. Therefore, these results suggested that, PTP1B inhibition might be involved in the amelioration of breast tumorigenesis. However, further extensive studies should be performed to support these findings. On the other hand, the structure activity relationships revealed that, hydroxy group at C-3 position or/and carboxy group at C-28 position increased both PTP1B inhibitory and cytotoxic activity in camellia oleananes while the attachment of ketone group at C-3 position was responsible for decrease in both type effect. Recent observations on some other triterpenes also agreed with these results. Therefore, based on the above findings, it is suggested that oleanane triterpenes from *C. japonica* as PTP1B inhibitors might be considered as potential anticancer molecules in breast cancer treatment.

5. References

1. Baselga, J.; Norton, L., Focus on breast cancer. *Cancer. Cell.* **2002**, 1, (4), 319-22.
2. American Cancer Society. In *Cancer Facts & Figures 2013*, Atlanta: American Cancer Society: 2013.
3. Stang, A.; Thomssen, C., Decline in breast cancer incidence in the United States: what about male breast cancer? *Breast. Cancer. Res.Tr.* **2008**, 112, (3), 595-96.
4. Key, T. J. A.; Pike, M. C., The role of oestrogens and progestagens in the epidemiology and prevention of breast cancer. *Eur. J. Cancer. Clin. On.* **1988**, 24, (1), 29-43.
5. Slamon, D.; Godolphin, W.; Jones, L.; Holt, J.; Wong, S.; Keith, D.; Levin, W.; Stuart, S.; Udove, J.; Ullrich, A.; et, a., Studies of the HER-2/neu proto-oncogene in human breast and ovarian cancer. *Science* **1989**, 244, (4905), 707-12.
6. Vogel, V., Chemoprevention strategies 2006. *Curr. Treat. Option. On.* **2007**, 8, (1), 74-88.
7. Powles, T. J.; Hickish, T.; Kanis, J. A.; Tidy, A.; Ashley, S., Effect of tamoxifen on bone mineral density measured by dual-energy x-ray absorptiometry in healthy premenopausal and postmenopausal women. *J. Clin. Oncol.* **1996**, 14, (1), 78-84.
8. Fisher, B.; Costantino, J. P.; Redmond, C. K.; Fisher, E. R.; Wickerham, D. L.; Cronin, W. M.; Contributors, O. N., Endometrial cancer in tamoxifen-treated breast cancer patients: findings from the national surgical adjuvant breast and bowel project (NSABP) B-14. *J. Natl. Cancer. I.* **1994**, 86, (7), 527-37.
9. Fisher, B.; Costantino, J. P.; Wickerham, D. L.; Redmond, C. K.; Kavanah, M.; Cronin, W. M.; Vogel, V.; Robidoux, A.; Dimitrov, N.; Atkins, J.; Daly, M.; Wieand,

S.; Tan-Chiu, E.; Ford, L.; Wolmark, N.; Breast, o. N. S. A.; Investigators, B. P., Tamoxifen for prevention of breast cancer: report of the national surgical adjuvant breast and bowel project P-1 study. *J. Natl. Cancer. I.* **1998**, 90, (18), 1371-88.

10. DeFriend, D.; Anderson, E.; Bell, J.; Wilks, D.; West, C.; Mansel, R.; Howell, A., Effects of 4-hydroxytamoxifen and a novel pure antioestrogen (ICI 182780) on the clonogenic growth of human breast cancer cells in vitro. *Brit. J. Cancer.* **1994**, 70, (2), 204.

11. Slamon, D.; Clark, G.; Wong, S.; Levin, W.; Ullrich, A.; McGuire, W., Human breast cancer: correlation of relapse and survival with amplification of the HER-2/neu oncogene. *Science* **1987**, 235, (4785), 177-82.

12. Cobleigh, M. A.; Vogel, C. L.; Tripathy, D.; Robert, N. J.; Scholl, S.; Fehrenbacher, L.; Wolter, J. M.; Paton, V.; Shak, S.; Lieberman, G.; Slamon, D. J., Multinational study of the efficacy and safety of humanized anti-HER2 monoclonal antibody in women who have HER2-overexpressing metastatic breast cancer that has progressed after chemotherapy for metastatic disease. *J. Clin. Oncol.* **1999**, 17, (9), 2639.

13. Chien, A. J.; Rugo, H. S., The cardiac safety of trastuzumab in the treatment of breast cancer. *Expert. Opin. Drug. Saf.* **2010**, 9, (2), 335-46.

14. Geyer, C. E.; Forster, J.; Lindquist, D.; Chan, S.; Romieu, C. G.; Pienkowski, T.; Jagiello-Gruszfeld, A.; Crown, J.; Chan, A.; Kaufman, B.; Skarlos, D.; Campone, M.; Davidson, N.; Berger, M.; Oliva, C.; Rubin, S. D.; Stein, S.; Cameron, D., Lapatinib plus capecitabine for HER2-positive advanced breast cancer. *New. Engl. J. Med.* **2006**, 355, (26), 2733-43.

15. Wong, J. S.; Harris, J. R., Importance of local tumour control in breast cancer. *Lancet. Oncol.* **2001**, 2, (1), 11-17.

16. Bange, J.; Zwick, E.; Ullrich, A., Molecular targets for breast cancer therapy and prevention. *Nat. Med.* **2001**, 7, (5), 548-52.

17. Loncaster, J.; Dodwell, D., Adjuvant radiotherapy in breast cancer. Are there factors that allow selection of patients who do not require adjuvant radiotherapy following breast-conserving surgery for breast cancer? *Minerva. Med.* **2002**, 93, (2), 101.

18. Ostman, A.; Hellberg, C.; Bohmer, F. D., Protein-tyrosine phosphatases and cancer. *Nat. Rev. Cancer.* **2006**, 6, (4), 307-20.

19. Tonks, N. K.; Diltz, C. D.; Fischer, E. H., Purification of the major protein-tyrosine-phosphatases of human placenta. *J. Biol. Chem.* **1988**, 263, (14), 6722-30.

20. Lessard, L.; Stuible, M.; Tremblay, M. L., The two faces of PTP1B in cancer. *BBA-Proteins. Proteom.* **2010**, 1804, (3), 613-19.

21. Barford, D.; Flint, A.; Tonks, N., Crystal structure of human protein tyrosine phosphatase 1B. *Science* **1994**, 263, (5152), 1397-404.

22. Kamerlin, S. C. L.; Rucker, R.; Boresch, S., A molecular dynamics study of WPD-loop flexibility in PTP1B. *Biochem. Bioph. Res. Co.* **2007**, 356, (4), 1011-16.

23. Jia, Z.; Barford, D.; Flint, A.; Tonks, N., Structural basis for phosphotyrosine peptide recognition by protein tyrosine phosphatase 1B. *Science* **1995**, 268, (5218), 1754-58.

24. Pedersen, A. K.; Guo, X.-L.; Møller, K. B.; Peters, G. H.; Andersen, H. S.; Kastrup, J. S.; Mortensen, S. B.; Iversen, L. F.; Zhang, Z.-Y.; Møller, N. P. H., Residue 182 influences the second step of protein-tyrosine phosphatase-mediated catalysis. *Biochem. J.* **2004**, 378, (2), 421-33.

25. Dubé, N.; Tremblay, M. L., Beyond the metabolic function of PTP1B. *Cell. Cycle.* **2004**, 3, (5), 548-51.

26. Bandyopadhyay, D.; Kusari, A.; Kenner, K. A.; Liu, F.; Chernoff, J.; Gustafson, T. A.; Kusari, J., Protein-tyrosine phosphatase 1B complexes with the insulin receptor in vivo and is tyrosine-phosphorylated in the presence of insulin. *J. Biol. Chem.* **1997**, 272, (3), 1639-45.

27. Kenner, K. A.; Anyanwu, E.; Olefsky, J. M.; Kusari, J., Protein-tyrosine phosphatase 1B Is a negative regulator of insulin- and insulin-like growth factor-I-stimulated signaling. *J. Biol. Chem.* **1996**, 271, (33), 19810-16.

28. Zinker, B. A.; Rondinone, C. M.; Trevillyan, J. M.; Gum, R. J.; Clampit, J. E.; Waring, J. F.; Xie, N.; Wilcox, D.; Jacobson, P.; Frost, L.; Kroeger, P. E.; Reilly, R. M.; Koterski, S.; Opgenorth, T. J.; Ulrich, R. G.; Crosby, S.; Butler, M.; Murray, S. F.; McKay, R. A.; Bhanot, S.; Monia, B. P.; Jirousek, M. R., PTP1B antisense oligonucleotide lowers PTP1B protein, normalizes blood glucose, and improves insulin sensitivity in diabetic mice. *P. Natl. Acad. Sci.* **2002**, 99, (17), 11357-62.

29. Elchebly, M.; Payette, P.; Michaliszyn, E.; Cromlish, W.; Collins, S.; Loy, A. L.; Normandin, D.; Cheng, A.; Himms-Hagen, J.; Chan, C.-C.; Ramachandran, C.; Gresser, M. J.; Tremblay, M. L.; Kennedy, B. P., Increased insulin sensitivity and obesity resistance in mice lacking the protein tyrosine phosphatase-1B gene. *Science* **1999**, 283, (5407), 1544-48.

30. Zabolotny, J. M.; Bence-Hanulec, K. K.; Stricker-Krongrad, A.; Haj, F.; Wang, Y.; Minokoshi, Y.; Kim, Y.-B.; Elmquist, J. K.; Tartaglia, L. A.; Kahn, B. B.; Neel, B. G., PTP1B regulates leptin signal transduction In vivo. *Dev. Cell.* **2002**, 2, (4), 489-95.

31. Bence, K. K.; Delibegovic, M.; Xue, B.; Gorgun, C. Z.; Hotamisligil, G. S.; Neel, B. G.; Kahn, B. B., Neuronal PTP1B regulates body weight, adiposity and leptin action. *Nat. Med.* **2006**, 12, (8), 917-24.

32. Bjorge, J. D.; Pang, A.; Fujita, D. J., Identification of protein-tyrosine phosphatase 1B as the major tyrosine phosphatase activity capable of dephosphorylating and activating c-Src in several human breast cancer cell lines. *J. Biol. Chem.* **2000**, 275, (52), 41439-46.

33. Julien, S. G.; Dube, N.; Read, M.; Penney, J.; Paquet, M.; Han, Y.; Kennedy, B. P.; Muller, W. J.; Tremblay, M. L., Protein tyrosine phosphatase 1B deficiency or inhibition delays ErbB2-induced mammary tumorigenesis and protects from lung metastasis. *Nat. Genet.* **2007**, 39, (3), 338-46.

34. Bentires-Alj, M.; Neel, B. G., Protein-tyrosine phosphatase 1B Is required for HER2/Neu–induced breast cancer. *Cancer. Res.* **2007**, 67, (6), 2420-24.

35. Tonks, N. K.; Muthuswamy, S. K., A Brake Becomes an Accelerator: PTP1B—A New Therapeutic Target for Breast Cancer. *Cancer Cell* **2007**, 11, (3), 214-16.

36. Yarden, Y., Biology of HER2 and its importance in breast cancer. *Oncology* **2001**, 61, 1.

37. Tanner, M. M.; Tirkkonen, M.; Kallioniemi, A.; Isola, J.; Kuukasjärvi, T.; Collins, C.; Kowbel, D.; Guan, X.-Y.; Trent, J.; Gray, J. W.; Meltzer, P.; Kallioniemi, O.-P., Independent amplification and frequent co-amplification of three nonsyntenic regions on the long arm of chromosome 20 in human breast cancer. *Cancer. Res.* **1996**, 56, (15), 3441-45.

38. Wiener, J. R.; Kerns, B.-J. M.; Harvey, E. L.; Conaway, M. R.; lglehart, J. D.; Berchuck, A.; Bast, R. C., Overexpression of the protien tyrosine phosphatase PTP1B in human breast cancer: assocation with p185c-erbB-2 protein expression. *J. Natl. Cancer. I.* **1994**, 86, (5), 372-78.

39. Tanner, M. M.; Grenman, S.; Koul, A.; Johannsson, O.; Meltzer, P.; Pejovic, T.; Borg, Å.; Isola, J. J., Frequent amplification of chromosomal region 20q12-q13 in ovarian cancer. *Clin. Cancer. Res.* **2000**, 6, (5), 1833-39.

40. Zhai, Y.-F.; Beittenmiller, H.; Wang, B.; Gould, M. N.; Oakley, C.; Esselman, W. J.; Welsch, C. W., Increased expression of specific protein tyrosine phosphatases in human breast epithelial cells neoplastically transformed by the neu oncogene. *Cancer. Res.* **1993**, 53, (10), 2272-78.

41. Liby, K. T.; Yore, M. M.; Sporn, M. B., Triterpenoids and rexinoids as multifunctional agents for the prevention and treatment of cancer. *Nat. Rev. Cancer.* **2007**, 7, (5), 357-69.

42. Phillips, D. R.; Rasbery, J. M.; Bartel, B.; Matsuda, S. P. T., Biosynthetic diversity in plant triterpene cyclization. *Curr. Opin. Plant. Biol.* **2006**, 9, (3), 305-14.

43. Petronelli, A.; Pannitteri, G.; Testa, U., Triterpenoids as new promising anticancer drugs. *Anti-Cancer. Drug.* **2009**, 20, (10), 880-92 10.1097/CAD.0b013e328330fd90.

44. Ovesna, Z.; Vachalkova, A.; Horvathova, K.; Tothova, D., Pentacyclic triterpenoic acids: new chemoprotective compounds. Minireview. *Neoplasma* **2004**, 51, (5), 327.

45. Thao, N. T. P.; Hung, T. M.; Lee, M. K.; Kim, J. C.; Min, B. S.; Bae, K., Triterpenoids from *Camellia japonica* and their cytotoxic activity. *Chem. Pharm. Bull.* **2010**, 58, (1), 121-24.

46. Setzer, W. N.; Setzer, M. C., Plant-derived triterpenoids as potential antineoplastic agents. *Mini-Rev. Med. Chem.* **2003**, 3, (6), 540-56.

47. Deng, Y.; Jiang, T.-Y.; Sheng, S.; Tianasoa-Ramamonjy, M.; Snyder, J. K., Remangilones A−C, new cytotoxic triterpenes from *Physena madagascariensis*. *J. Nat. Prod.* **1999**, 62, (3), 471-76.

48. Hsu, H.-F.; Houng, J.-Y.; Chang, C.-L.; Wu, C.-C.; Chang, F.-R.; Wu, Y.-C., Antioxidant activity, cytotoxicity, and DNA Information of *Glossogyne tenuifolia*. *J. Agric. Food. Chem.* **2005**, 53, (15), 6117-25.

49. Es-Saady, D.; Simon, A.; Jayat-Vignoles, C.; Chulia, A. J.; Delage, C., MCF-7 cell cycle arrested at G1 through ursolic acid, and increased reduction of tetrazolium salts. *Anticancer. Res.* **1996**, 16, (1), 481-86.

50. Neto, C. C.; Vaisberg, A. J.; Zhou, B.-N.; Kingston, D. G.; Hammond, G. B., Cytotoxic triterpene acids from the Peruvian medicinal plant *Polylepis racemosa*. *Planta. Med.* **2000**, 66, (05), 483-84.

51. Murphy, B. T.; MacKinnon, S. L.; Yan, X.; Hammond, G. B.; Vaisberg, A. J.; Neto, C. C., Identification of triterpene hydroxycinnamates with in vitro antitumor activity from whole cranberry fruit (*Vaccinium macrocarpon*). *J. Agric. Food. Chem.* **2003**, 51, (12), 3541-45.

52. Setzer, W. N.; Setzer, M. C.; Bates, R. B.; Jackes, B. R., Biologically active triterpenoids of *Syncarpia glomulifera* bark extract from Paluma, north Queensland, Australia. *Planta. Med.* **2000**, 66, (02), 176-77.

53. Rzeski, W.; Stepulak, A.; Szymański, M.; Juszczak, M.; Grabarska, A.; Sifringer, M.; Kaczor, J.; Kandefer-Szerszeń, M., Betulin elicits anti-cancer effects in tumour primary cultures and cell lines In vitro. *Basic. Clin. Pharmacol.* **2009**, 105, (6), 425-32.

54. Lambertini, E.; Lampronti, I.; Penolazzi, L.; Khan, M. T. H.; Ather, A.; Giorgi, G.; Gambari, R.; Piva, R., Expression of estrogen receptor gene in breast cancer cells treated with transcription factor decoy Is modulated by Bangladeshi natural plant extracts. *Oncol. Res.* **2005**, 15, (2), 69-79.

55. Blaskovich, M. A.; Sun, J.; Cantor, A.; Turkson, J.; Jove, R.; Sebti, S. M., Discovery of JSI-124 (cucurbitacin I), a selective janus kinase/signal transducer and activator of transcription 3 signaling pathway inhibitor with potent antitumor activity against human and murine cancer cells in mice. *Cancer. Res.* **2003**, 63, (6), 1270-79.

56. Rodriguez, N.; Vasquez, Y.; Hussein, A. A.; Coley, P. D.; Solis, P. N.; Gupta, M. P., Cytotoxic cucurbitacin constituents from *Sloanea zuliaensis*. *J. Nat. Prod.* **2003**, 66, (11), 1515-16.

57. Jayaprakasam, B.; Seeram, N. P.; Nair, M. G., Anticancer and antiinflammatory activities of cucurbitacins from *Cucurbita andreana*. *Cancer. Lett.* **2003**, 189, (1), 11-16.

58. Kitamura, S.; Murata, G., *Colored illustrations of woody plants of Japan*. Hoikusha Pub.: 1980.

59. Yoshikawa, M.; Murakami, T.; Yoshizumi, S.; Murakami, N.; Yamahara, J.; Matsuda, H., Bioactive saponins and glycosides. V. Acylated polyhydroxyolean-12-ene triterpene oligoglycosides, camelliasaponins A_1, A_2, B_1, B_2, C_1, and C_2, from the seeds of *Camellia japonica* L. : structures and Inhibitory activity on alcohol absorption. *Chem. Pharm. Bull.* **1996**, 44, (10), 1899-907.

60. Yoshikawa, M.; Morikawa, T.; Asao, Y.; Fujiwara, E.; Nakamura, S.; Matsuda, H., Medicinal flowers. XV. The structures of noroleanane- and oleanane-type triterpene oligoglycosides with gastroprotective and platelet aggregation activities from flower buds of *Camellia japonica*. *Chem. Pharm. Bull.* **2007**, 55, (4), 606-12.

61. Itô, S.; Kodama, M.; Konoike, M., Structure of camelliagenins. *Tetrahedron. Lett.* **1967**, 8, (7), 591-96.

62. Itokawa, H.; Sawada, N.; Murakami, T., The structures of camelliagenin A, B, and C obtained from *Camellia japonica* L. *Tetrahedron. Lett.* **1967**, 8, (7), 597-601.

63. Itokawa, H.; Sawada, N.; Murakami, T., The structures of camelliagenin A, B and C obtained from *Camellia japonica* L. *Chem. Pharm. Bull.* **1969**, 17, (3), 474-80.

64. Yoshikawa, M.; Harada, E.; Murakami, T.; Matsuda, H.; Yamahara, J.; Murakami, N., Camellia saponins B_1, B_2, C_1 and C_2, new type inhibitors of ethanol absorption in rats from the seeds of *Camellia japonica* L. *Chem. Pharm. Bull.* **1994**, 42, (3), 742-44.

65. Onodera, K.-i.; Hanashiro, K.; Yasumoto, T., Camellianoside, a novel antioxidant glycoside from the leaves of *Camellia japonica*. *Biosci. Biotech. Bioch.* **2006**, 70, (8), 1995-98.

66. Yoshida, T.; Chou, T.; Maruyama, Y.; Okuda, T., Tannins of theaceous plants. II. : camelliins A and B, two new dimeric hydrolyzable tannins from flower buds of *Camellia japonica* L. and *Camellia sasanqua* Thumb. *Chem. Pharm. Bull.* **1990**, 38, (10), 2681-86.

67. Saito, N.; Yokoi, M.; Yamaji, M.; Honda, T., Cyanidin 3-p-coumaroylglucoside in Camellia species and cultivars. *Phytochemistry* **1987**, 26, (10), 2761-62.

68. Itokawa, H.; Nakajima, H.; Ikuta, A.; Iitaka, Y., Two triterpenes from the flowers of *Camellia japonica*. *Phytochemistry* **1981**, 20, (11), 2539-42.

69. Fujimori, N.; Ashihara, H., Adenine metabolism and the synthesis of purine alkaloids in flowers of Camellia. *Phytochemistry* **1990**, 29, (11), 3513-16.

70. Akihisa, T.; Yasukawa, K.; Kimura, Y.; Takase, S.-i.; Yamanouchi, S.; Tamura, T., Triterpene alcohols from camellia and sasanqua oils and their anti-inflammatory effects. *Chem. Pharm. Bull.* **1997**, 45, (12), 2016-23.

71. Numata, A.; Kitajima, A.; Katsuno, T.; Yamamoto, K.; Nagahama, N.; Takahashi, C.; Fujiki, R.; Nabae, M., An antifeedant for the yellow butterfly larvae in *Camellia Japonica*: a revised structure of camellidin II. *Chem. Pharm. Bull.* **1987**, 35, (9), 3948-51.

72. Park, J. C.; Hur, J. M.; Park, J. G.; Hatano, T.; Yoshida, T.; Miyashiro, H.; Min, B. S.; Hattori, M., Inhibitory effects of Korean medicinal plants and camelliatannin H from *Camellia japonica* on human immunodeficiency virus type 1 protease. *Phytother. Res.* **2002**, 16, (5), 422-26.

73. Hatano, T.; Han, L.; Taniguchi, S.; Shingu, T.; Okuda, T.; Yoshida, T., Tannins and related polyphenols of theaceous plants. VIII. camelliatannins C and E, new complex tannins from *Camellia japonica* leaves. *Chem. Pharm. Bull.* **1995**, 43, (10), 1629-33.

74. Hatano, T.; Shida, S.; Han, L.; Okuda, T., Tannins of theaceous plants. III. camelliatannins A and B, two new complex tannins from *Camellia japonica* L. *Chem. Pharm. Bull.* **1991**, 39, (4), 876-80.

75. Cui, L.; Na, M.; Oh, H.; Bae, E. Y.; Jeong, D. G.; Ryu, S. E.; Kim, S.; Kim, B. Y.; Oh, W. K.; Ahn, J. S., Protein tyrosine phosphatase 1B inhibitors from Morus root bark. *Bioorg. Med. Chem. Lett.* **2006**, 16, (5), 1426-29.

76. Dixon, M., The determination of enzyme inhibitor constants. *Biochem. J.* **1953**, 55, (1), 170-71.

77. Lineweaver, H.; Burk, D., The determination of enzyme dissociation constants. *J. Am. Chem. Soc.* **1934**, 56, (3), 658-66.

78. Hussain, R. F.; Nouri, A. M. E.; Oliver, R. T. D., A new approach for measurement of cytotoxicity using colorimetric assay. *J. Immunol. Methods.* **1993**, 160, (1), 89-96.

79. Ikuta, A.; Kamiya, K.; Satake, T.; Saiki, Y., Triterpenoids from callus tissue cultures of *Paeonia species*. *Phytochemistry* **1995**, 38, (5), 1203-07.

80. Caldwell, C. G.; Franzblau, S. G.; Suarez, E.; Timmermann, B. N., Oleanane triterpenes from *Junellia tridens*. *J. Nat. Prod.* **2000**, 63, (12), 1611-14.

81. Kwon, J.-H.; Chang, M.-J.; Seo, H.-W.; Lee, J.-H.; Min, B.-S.; Na, M.; Kim, J. C.; Woo, M. H.; Choi, J. S.; Lee, H. K.; Bae, K., Triterpenoids and a sterol from the stem-bark of *Styrax japonica* and their protein tyrosine phosphatase 1B inhibitory activities. *Phytother. Res.* **2008**, 22, (10), 1303-06.

82. Chiang, Y.-M.; Kuo, Y.-H., New peroxy triterpenes from the aerial roots of *Ficus microcarpa*. *J. Nat. Prod.* **2001**, 64, (4), 436-39.

83. Kobayashi, Y.; Ogihara, Y., New triterpenoids from the leaves of *Bupleurum rotundifolium* L. *Chem. Pharm. Bull.* **1981**, 29, (8), 2230-36.

84. Seebacher, W.; Simic, N.; Weis, R.; Saf, R.; Kunert, O., Complete assignments of 1H and 13C NMR resonances of oleanolic acid, 18α-oleanolic acid, ursolic acid and their 11-oxo derivatives. *Magn. Reson. Chem.* **2003**, 41, (8), 636-38.

85. Kagawa, M.; Minami, H.; Nakahara, M.; Takahashi, H.; Takaoka, S.; Fukuyama, Y., Oleanane-type triterpenes from *Viburnum awabuki*. *Phytochemistry* **1998**, 47, (7), 1337-41.

86. Nakamura, S.; Moriura, T.; Park, S.; Fujimoto, K.; Matsumoto, T.; Ohta, T.; Matsuda, H.; Yoshikawa, M., Melanogenesis inhibitory and fibroblast proliferation accelerating effects of noroleanane- and oleanane-type triterpene oligoglycosides from the flower buds of *Camellia japonica*. *J. Nat. Prod.* **2012**, 75, (8), 1425-30.

87. Kaneda, N.; Pezzuto, J. M.; Kinghorn, A. D.; Farnsworth, N. R.; Santisuk, T.; Tuchinda, P.; Udchachon, J.; Reutrakul, V., Plant anticancer agents, L. cytotoxic triterpenes from *Sandoricum koetjape* Stems. *J. Nat. Prod.* **1992**, 55, (5), 654-59.

88. Thuong, P. T.; Lee, C. H.; Dao, T. T.; Nguyen, P. H.; Kim, W. G.; Lee, S. J.; Oh, W. K., Triterpenoids from the leaves of *Diospyros kaki* (persimmon) and their inhibitory effects on protein tyrosine phosphatase 1B. *J. Nat. Prod.* **2008**, 71, (10), 1775-78.

89. Tonks, N. K.; Muthuswamy, S. K., A brake becomes an accelerator: PTP1B—a new therapeutic target for breast cancer. *Cancer. Cell.* **2007**, 11, (3), 214-16.

90. Efdi, M.; Ninomiya, M.; Suryani, E.; Tanaka, K.; Ibrahim, S.; Watanabe, K.; Koketsu, M., Sentulic acid: a cytotoxic ring A-seco triterpenoid from *Sandoricum koetjape* Merr. *Bioorg. Med. Chem. Lett.* **2012**, 22, (13), 4242-45.

91. Mallavadhani, U. V.; Mahapatra, A.; Jamil, K.; Reddy, P. S., Antimicrobial activity of some pentacyclic triterpenes and their synthesized 3-*O*-lipophilic chains. *Biol. Pharm. Bull.* **2004**, 27, (10), 1576-79.

92. Na, M.; Cui, L.; Min, B. S.; Bae, K.; Yoo, J. K.; Kim, B. Y.; Oh, W. K.; Ahn, J. S., Protein tyrosine phosphatase 1B inhibitory activity of triterpenes isolated from *Astilbe koreana*. *Bioorg. Med. Chem. Lett.* **2006**, 16, (12), 3273-76.

93. Akihisa, T.; Tokuda, H.; Ichiishi, E.; Mukainaka, T.; Toriumi, M.; Ukiya, M.; Yasukawa, K.; Nishino, H., Anti-tumor promoting effects of multiflorane-type triterpenoids and cytotoxic activity of karounidiol against human cancer cell lines. *Cancer. Lett.* **2001**, 173, (1), 9-14.

94. Chiang, Y.-M.; Chang, J.-Y.; Kuo, C.-C.; Chang, C.-Y.; Kuo, Y.-H., Cytotoxic triterpenes from the aerial roots of *Ficus microcarpa*. *Phytochemistry* **2005**, 66, (4), 495-501.

6. Acknowledgements

This thesis would not have been possible without the support, both scientific and personal, of a great many people. Foremost, I would like to express my sincerest gratitude to my advisor, Prof. Choi Hong Seok and co-advisor, Prof. Oh Won Keun, who brought me into research world. Their encouragement, enthusiasm and perpetual demand for excellence, both scientifically and professionally, have been the mainstay of my inspiration throughout my work. I cannot figure out appropriate words to express how thankful and admirable I am to my great professors.

In completing the course I have also been particularly impressed with the boundless helps of our lab members, Yang Jun-Li, Sharma Govinda, Dhodhary Basanta, Ha Thi Kim Quy, Kim Kuk Hwa. Also special thanks to former lab members, Dao Trong Tuan, Nguyen Phi Hung and Kim Ja Yeon. I am grateful to them for their excellent assistance and significant contribution.

I would also like to express my gratitude to all professors at College of Pharmacy, Chosun University for their invaluable mentoring, support and emotional encouragement during my graduate training.

Finally, my love and gratefulness go to my parents, without whom I would not have had the opportunity to embark on this journey and fulfill my childhood ambitions of a scientific career. I would like to express my special thanks to them for their patience, constant encouragement, and enthusiasm which have sustained my endeavor to complete the work.

Korea, May, 2013

Uddin Mohammad Nasir

저작물 이용 허락서

학 과	약학대학	학 번	20117755	과 정	석사
성 명	한글: 우딘 모함마드 나시르 영문: Uddin Mohammad Nasir				
주 소	501-759 광주광역시 동구 서석동 375 조선대학교 약학과 천연물화학실험실				
연락처	E-MAIL: nasiruddin1286@gmail.com				
논문제목	한글: 동백나무로부터 분리한 올레안계 화합물의 PTP1B 효소 저해를 경유한 유방암 세포주 저해활성 연구 영문: Oleanane triterpenes from *Camellia japonica* inhibit growth of breast cancer cell lines via PTP1B inhibition				

본인이 저작한 위의 저작물에 대하여 다음과 같은 조건 아래 -조선대학교가 저작물을 이용할 수 있도록 허락하고 동의합니다.

- 다 음 -

1. 저작물의 DB구축 및 인터넷을 포함한 정보통신망에의 공개를 위한 저작물의 복제, 기억장치에의 저장, 전송 등을 허락함

2. 위의 목적을 위하여 필요한 범위 내에서의 편집・형식상의 변경을 허락함.
다만, 저작물의 내용변경은 금지함.

3. 배포・전송된 저작물의 영리적 목적을 위한 복제, 저장, 전송 등은 금지함.

4. 저작물에 대한 이용기간은 5년으로 하고, 기간종료 3개월 이내에 별도의 의사표시가 없을 경우에는 저작물의 이용기간을 계속 연장함.

5. 해당 저작물의 저작권을 타인에게 양도하거나 또는 출판을 허락을 하였을 경우에는 1개월 이내에 대학에 이를 통보함.

6. 조선대학교는 저작물의 이용허락 이후 해당 저작물로 인하여 발생하는 타인에 의한 권리 침해에 대하여 일체의 법적 책임을 지지 않음

7. 소속대학의 협정기관에 저작물의 제공 및 인터넷 등 정보통신망을 이용한 저작물의 전송・출력을 허락함.

2013 년 8월 23일

동의 여부: 동의 () 조건부 동의(O) 반대 ()

저작자: 우딘 모함마드 나시르 (서명 또는 인)

조선대학교 총장 귀하

This thesis is examined and approved for

Uddin Mohammad Nasir's master degree

Chairman Chosun Univ. Prof. Choi Hoo Kyun (인)

Member Seoul National Univ. Prof. Kang Keon Wook (인)

Member Chosun Univ. Prof. Choi Hong Seok (인)

2013년 05월

Chosun University Graduate School